

Electronic Supplementary Information

Aggregation induced emission enhancement and growth of naphthalimide nanoribbons via J-aggregation: Insight into disaggregation induced unfolding and detection of ferritin at nanomolar level†

Niranjan Meher,^a Sayan Roy Chowdhury^a and Parameswar Krishnan Iyer^{*a,b}

^aDepartment of Chemistry, ^bCenter for Nanotechnology, Indian Institute of Technology Guwahati, Guwahati-781039, Assam, India

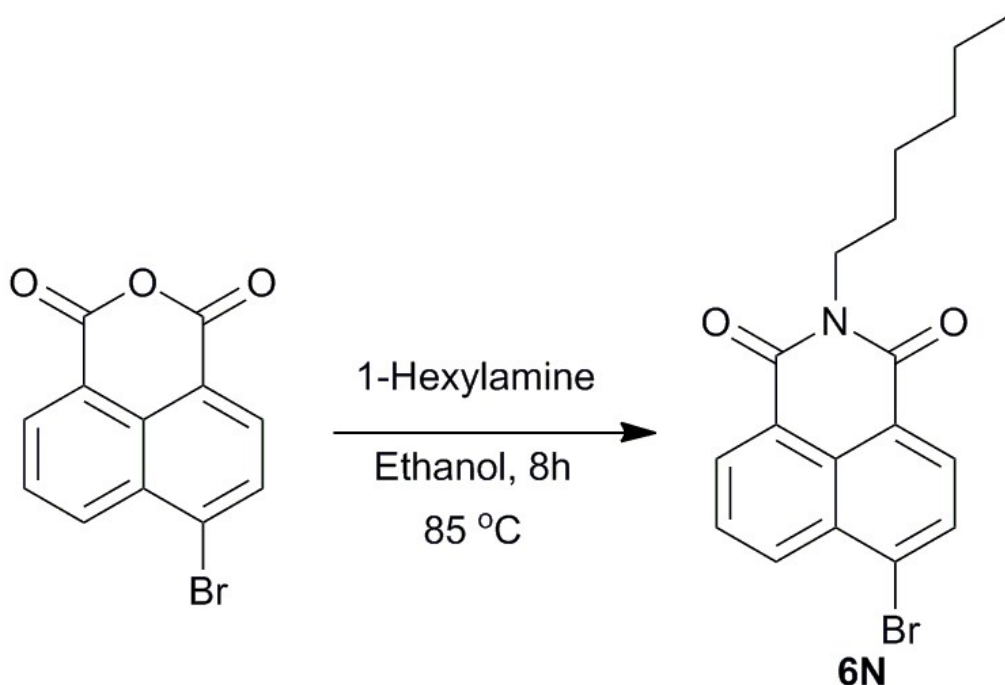
E-mail: pki@iitg.ernet.in

Table of Contents:	Page No.
1. Synthesis of Compounds	S3
2. Study of photophysical properties	S7
3. Study of AIEE Properties	S10
4. Time-Resolved Photoluminescence Study	S13
5. DLS Studies of Aggregates of α -NQ, α -NN and β -NN	S15
6. X-ray Structures and data of α -NQ and β -NN	S16
7. Computational Methods	S18
8. AFM Images of aggregates of α -NQ, α -NN and β -NN	S25
9. FE-SEM and TEM Images of aggregates α -NQ	S27
10. Sensing studies and calculations	S28
10. ¹ H-NMR, ¹³ C-NMR and Mass Spectra	S35
11. References	S41

Materials and methods, instrumentation, and measurements

All starting materials, reagents and protein analytes (viz: 4-bromo-1,8-naphthalene anhydride, 8-hydroxyquinoline, hexylamine, α -naphthol, β -naphthol, ferritin, hemin, Cc, MetHb, BSA, Vit B₁₂, insulin, casein, RNase) were purchased from Sigma Aldrich (INDIA) and were of reagent grade. HPLC grade solvents were purchased from Zenith India and Northeast Chemicals. NMR (¹H, ¹³C) spectra were recorded with a Varian-AS400 NMR spectrometer or Bruker Avance 600 MHz spectrometer. All solutions for ¹H and ¹³C spectra were obtained taking residual solvent signal as internal reference. Electro spray ionization mass (ESI-MS) spectra were recorded on a Waters (Micro mass MS-Technologies) Q-ToF MS Analyzer spectrometer. Microbalance (\pm 0.1mg) and volumetric glassware were used for the preparation of solutions. UV/vis and PL spectra were recorded on a Perkin-Elmer Model Lambda-750 spectrophotometer and a Horiba Fluoromax-4 spectrofluorometer respectively using 4 mm quartz cuvettes at 298 K. Fluorescence quantum yields in solutions were determined by standard methods using Quinine sulphate ($\Phi_F = 0.577$ in 0.1 M H₂SO₄, $\lambda_{ex} = 350$ nm). Solid state absorbance and emission were recorded with Fluoromax-4 fluorescence spectrophotometer equipped with a Quanta- ϕ integrating sphere for solid state fluorescence quantum yield. Malvern Zetasizer instrument was used to measure the hydrodynamic diameter of the compounds. Life-time measurements were performed using a MicroTime-200 instrument. Single crystal data were obtained with a Bruker SMART APEX diffractometer equipped with a CCD area detector. The data integration and reduction were processed with SAINT¹. SHELXL-97² was used for the structure solutions via direct method and refined by full-matrix least-squares on F². TEM, FE-SEM and AFM samples were made using drop-cast method from 99.9% Water / 0.1% DMF solvent mixtures and were left for drying at room temperature. Atomic force microscopy images were recorded on an Agilent 5500-AFM/STM instrument. FE-SEM-images were obtained on Sigma Carl ZEISS field emission scanning electron microscope. TEM images were collected from a JEOL 2100 UHR-TEM instrument, operating at 200 KV. CD spectra were recorded on a JASCO, J-815 CD Spectrometer, model no. J-815-150S. Changes in the secondary structure of metalloproteins were recorded in the far UV region (190 – 240 nm) using 0.4 cm path length cells and 20 nm min⁻¹ scan speed.

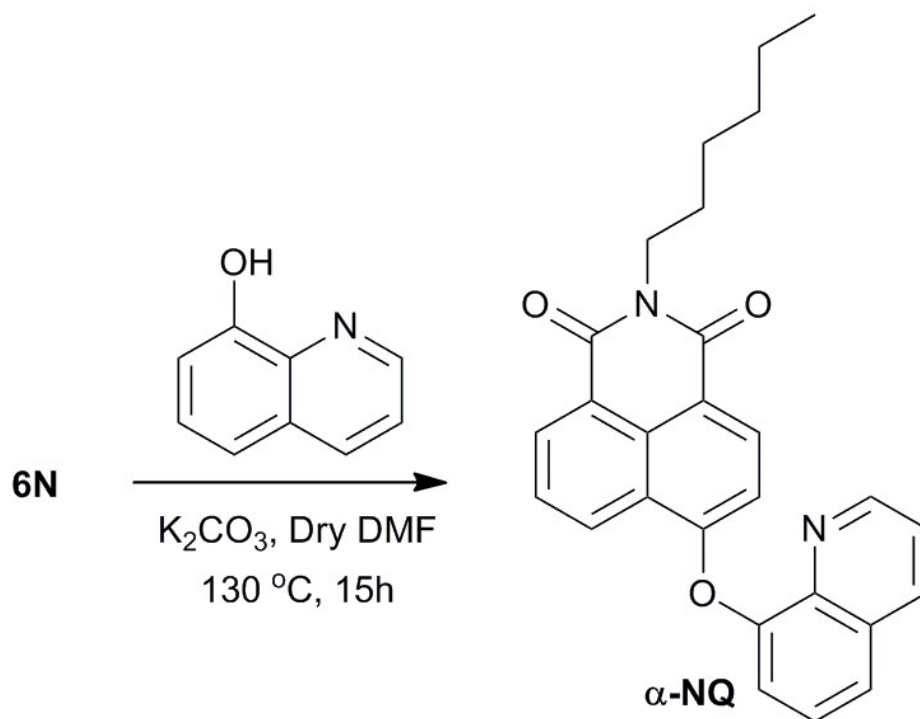
1. Synthesis of Compounds



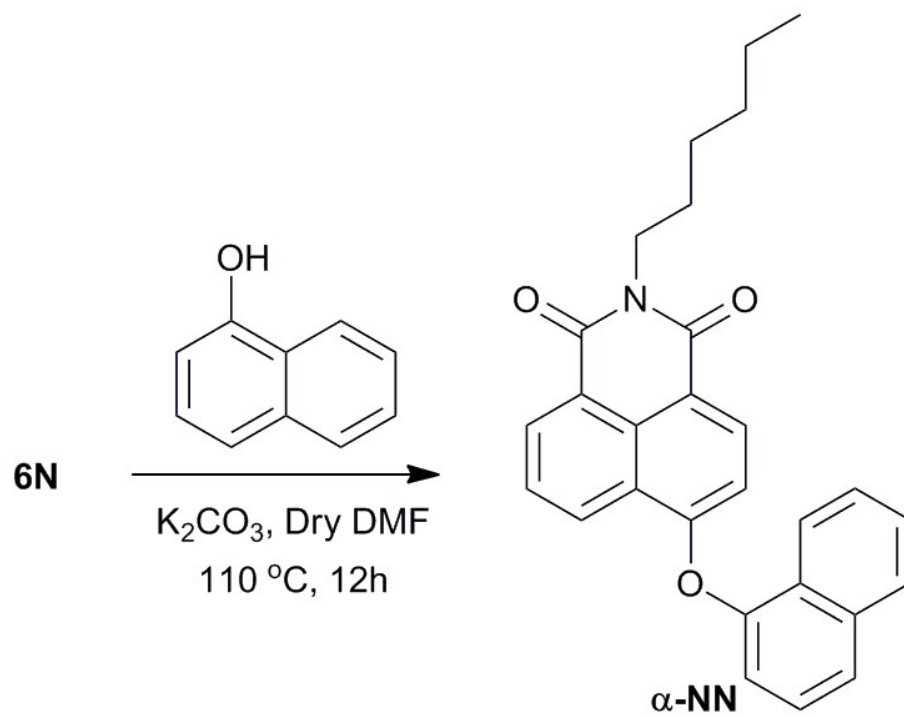
Scheme S1: Synthesis of **6N**

Compound 6N. 4-bromo-1,8-naphthalic anhydride (554.2 mg, 2 m.mol) was taken in ethanol (20 mL) and hexylamine (202.38 mg, 2 m.mol) was added to it at room temperature. The suspension was heated at 85 °C with vigorous stirring for 8h. Then the mixture was cooled to room temperature and evaporated under reduced pressure. The mixture was extracted with chloroform and washed with water. Then it was dried over anhydrous Na₂SO₄ and concentrated. After that it was finally purified by column over silica gel with 2% ethyl acetate in hexane as eluent which gives pure **2**.

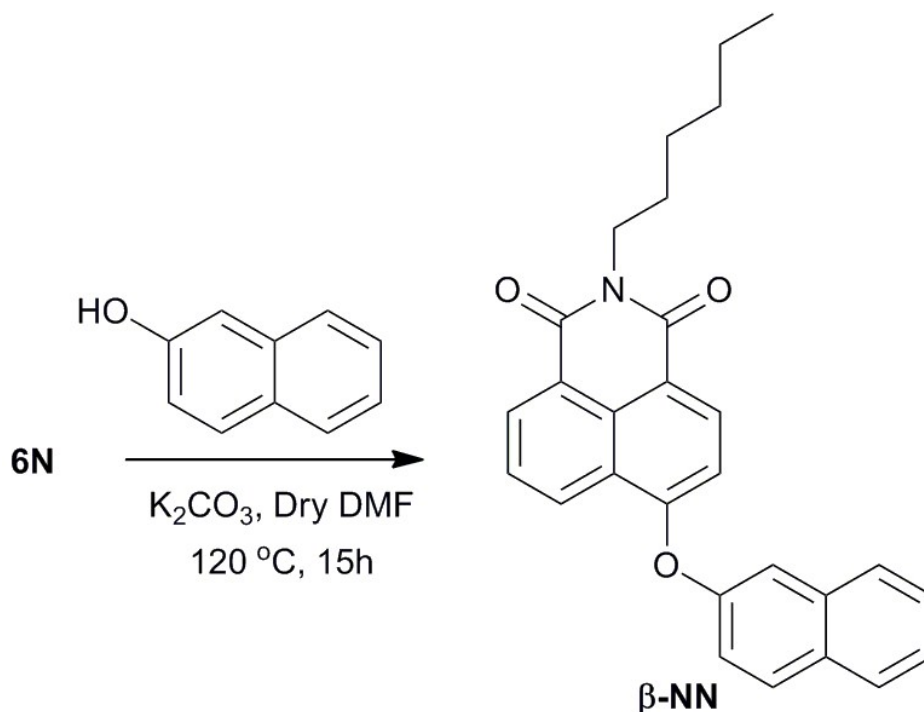
Compound 6N: Light green solid (630 mg, 83% yield). ¹H NMR (400 MHz, CDCl₃, δ ppm) 0.87 (t, *J* = 8.0 Hz, 3H), 1.31 (m, *J* = 8.0 Hz, 6H), 1.70 (m, *J* = 8.0 Hz, 2H), 4.12 (t, *J*=8.0 Hz,3H) 7.77 (t, *J* = 8.0 Hz, 1H), 7.94 (d, *J* = 8.0 Hz, 1H), 8.32 (d, *J* = 8.0 Hz, 1H), 8.46 (d, *J* = 8.0 Hz, 1H), 8.57 (d, *J*=8 Hz, 1H). ¹³C NMR (100.00 MHz, CDCl₃, δ ppm) 14.25, 22.74, 26.96, 28.18, 31.71, 40.78, 122.34, 123.21, 128.15, 128.98, 130.24, 130.61, 131.16, 131.25, 132.06, 133.22, 163.60, 163.63. HRMS (+ESI): Calculated for C₁₈H₁₈BrNO₂ 359.0521 [M]⁺, 361.0500[M+2]⁺, Found 360.0600 [M+H]⁺, 362.0581 [M+H+2]⁺.



Scheme S2: Synthesis of α -NQ



Scheme S3: Synthesis of α -NN



Scheme S4: Synthesis of **β -NN**

Compounds, α -NQ, α -NN and β -NN. To a solution of **6N** (0.5 mmol) in dry DMF (10 mL), 0.7 mmol of 8-hydroxyquinoline (for **α -NQ**)/ α -naphthol (for **α -NN**)/ β -naphthol (for **β -NN**) and of K_2CO_3 (300 mg) were added and the mixture was heated at 110-130 °C for 15 hours with vigorous stirring. The solvent was evaporated under vacuum and the residue was extracted with chloroform (40×5 mL). The organic layer was washed with H_2O for several times followed by washing with brine. The organic layer was dried over anhydrous Na_2SO_4 and mixture was concentrated under reduced pressure to get crude product. Further purification was done by column chromatography over silica gel increasing the polarity slowly using mixture of hexane and chloroform to get the pure products as **α -NQ**, **α -NN** and **β -NN** respectively.

Compound α -NQ: Yellow solid (145 mg, 68 % yield). ^1H NMR (400 MHz, CDCl_3 , δ ppm) 0.86 (t, $J = 8.0$ Hz, 3H), 1.32 (m, $J = 8.0$ Hz, 6H), 1.70 (m, $J = 8.0$ Hz, 2H), 4.14 (t, $J=8.0$ Hz, 3H), 6.72(d, $J=8.00$ Hz, 1H), 7.46 (d, $J = 8.0$ Hz, 2H), 7.57 (t, $J = 8.0$ Hz, 1H), 7.76-7.79 (m, 2H), 8.24 (d, $J = 8.0$ Hz, 1H), 8.37 (d, $J=8.0$ Hz, 1H), 8.64 (d, $J = 8.0$ Hz, 1H), 8.85 (d, $J=8.0$ Hz, 2H). ^{13}C NMR (100.00 MHz, CDCl_3 , δ ppm) 14.25, 22.73, 26.97, 28.25, 31.72, 40.53, 111.39, 116.84, 120.32, 122.29, 122.72, 123.91, 125.63, 126.62, 126.89, 129.16, 129.81, 130.24, 131.95, 132.84, 136.42, 141.31, 150.91, 151.11, 160.51, 163.93, 164.58. HRMS (+ESI): Calculated for $\text{C}_{27}\text{H}_{24}\text{N}_2\text{O}_3$ 424.1787 $[\text{M}]^+$, Found 425.1894 $[\text{M}+\text{H}]^+$.

Compound α -NN: Light brown solid (158 mg, 74 % yield). ^1H NMR (400 MHz, CDCl_3 , δ ppm) 0.88 (t, $J = 8.0$ Hz, 3H), 1.25-1.41 (m, $J = 8.0$ Hz, 4H), 1.62 (m, $J = 8.0$ Hz, 2H), 1.72 (m, $J = 8.0$ Hz, 2H) 4.16 (t, $J = 8.0$ Hz, 3H), 6.77(d, $J = 8.00$ Hz, 1H), 7.27 (d, $J = 8.0$ Hz, 1H), 7.45 (t, $J = 8.0$ Hz, 1H), 7.52-7.58 (m, 2H), 7.82-7.86 (m, 2H), 7.92-7.97 (m, 2H), 8.38 (d, $J = 8.0$ Hz, 1H), 8.70 (d, $J = 8.0$ Hz, 2H), 8.88 (d, $J = 8.0$ Hz, 2H). ^{13}C NMR (100.00 MHz, CDCl_3 , δ ppm) 14.10, 22.59, 26.82, 28.09, 31.58, 40.42, 110.31, 116.61, 116.90, 121.44, 122.74, 123.54, 125.90, 125.91, 126.63, 126.73, 126.75, 126.99, 128.24, 128.47, 129.71, 131.91, 132.91, 135.21, 150.36, 160.19, 163.73, 164.41. HRMS (+ESI): Calculated for $\text{C}_{27}\text{H}_{24}\text{N}_2\text{O}_3$ 423.1834 $[\text{M}]^+$, Found 424.1926 $[\text{M}+\text{H}]^+$.

Compound β -NN: Olive green solid (165 mg, 77 % yield). ^1H NMR (400 MHz, CDCl_3 , δ ppm) 0.89 (t, $J = 8.0$ Hz, 3H), 1.33 (m, $J = 8.0$ Hz, 6H), 1.74 (m, $J = 8.0$ Hz, 2H), 4.17 (t, $J = 8.0$ Hz, 3H), 6.92(d, $J = 8.00$ Hz, 1H), 7.33 (d, $J = 8.0$ Hz, 1H), 7.49-7.52 (m, $J = 8.0$ Hz, 2H), 7.59 (s, 1H), 7.72-7.79 (m, $J = 8.0$ Hz, 2H), 7.88 (d, $J = 8.0$ Hz, 1H), 7.94 (d, $J = 8.0$ Hz, 1H), 8.41 (d, $J = 8.0$ Hz, 1H), 8.62 (d, $J = 8.0$ Hz, 1H), 8.70 (d, $J = 8.0$ Hz, 1H). ^{13}C NMR (100.00 MHz, CDCl_3 , δ ppm) 14.14, 22.62, 26.85, 28.12, 31.59, 40.47, 110.88, 116.62, 117.35, 120.38, 122.54, 123.83, 125.85, 126.51, 127.01, 127.44, 127.92, 128.50, 129.56, 130.66, 131.19, 131.85, 132.75, 134.22, 152.35, 159.78, 163.70, 164.32. HRMS (+ESI): Calculated for $\text{C}_{27}\text{H}_{24}\text{N}_2\text{O}_3$ is 423.1834 $[\text{M}]^+$, Found 424.1910 $[\text{M}+\text{H}]^+$.

2. Study of photophysical properties

Table S1. Photophysical properties of α -NQ, α -NN and β -NN various solvents at 10 μ M concentration.

Compound	Solvent	$\lambda_{\text{abs. max}}$ [nm]	ϵ^a [M ⁻¹ cm ⁻¹]	$\lambda_{\text{em. max}}^b$ [nm]	Stokes shift $\Delta\lambda/\text{nm}$	$\Phi_{\text{FL}} [\%]^c$
α -NQ	Hexane	357	24816	412	55	5.72
	Toluene	361	21167	422	61	29.71
	DCM	362	22785	432	70	37.67
	THF	360	21371	427	67	31.14
	CHCl ₃	362	22120	430	68	50.69
	EtOAc	359	22813	429	70	35.32
	CH ₃ OH	361	21890	442	81	1.84
	CH ₃ CN	359	21424	439	80	3.66
	DMF	361	20194	437	76	3.50
	DMSO	364	22461	440	76	3.74
	H ₂ O	370	15550	502	132	2.93
α -NN	Hexane	356	16885	412	56	15.74
	Toluene	360	14561	434	74	1.78
	DCM	362	17170	471	109	2.55
	THF	360	14685	435	75	2.39
	CHCl ₃	356	16087	411	55	8.27
	EtOAc	357	17809	430	73	10.72
	CH ₃ OH	356	16050	426	70	1.01
	CH ₃ CN	359	17614	435	76	0.78
	DMF	360	15051	432	72	1.95
	DMSO	362	15154	439	77	2.26
	H ₂ O	387	14543	483	96	3.76
β -NN	Hexane	356	18683	408	52	28.33
	Toluene	361	14521	422	61	14.49

DCM	363	19690	463	100	3.75
THF	364	20807	440	76	2.78
CHCl ₃	363	20790	414	51	3.04
EtOAc	359	23243	431	72	8.14
CH ₃ OH	362	21461	430	68	0.68
CH ₃ CN	359	23743	432	73	0.87
DMF	362	21536	433	71	1.09
DMSO	363	21876	439	76	1.31
H ₂ O	390	14270	494	104	3.39

^aMeasured at each absorption maximum. ^bExcited at 360 nm for all compounds. ^cQuantum yields were calculated by using quinine sulfate (0.1 M H₂SO₄, $\lambda_{\text{ex}} = 350$ nm, $\Phi_{\text{FL}} = 57.7\%$) solution as reference together with the following formula: $\Phi_{\text{FL}} = \Phi_{\text{FL}}(I/I_{\text{R}})(A_{\text{R}}/A)(\eta^2/\eta_{\text{R}}^2)$, where Φ = quantum yield, I = intensity of emission, A = absorbance at λ_{ex} , η = refractive index of solvent, R = reference. (10 μM)

Absorption and normalized emission spectra of α -NQ, α -NN and β -NN in various solvents

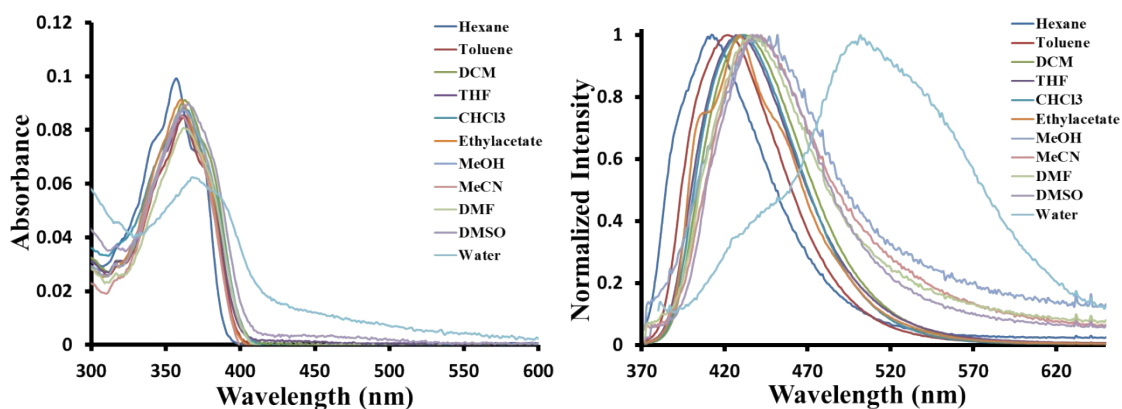


Figure S1. Absorption (left) and normalized emission spectra (right) of α -NQ (10 μM) in various solvents at 25 °C. $\lambda_{\text{ex}} = 360$ nm.

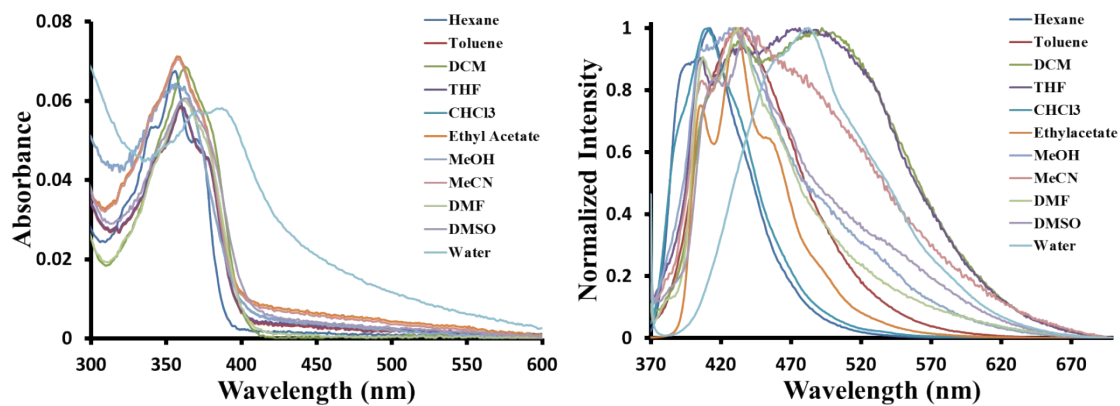


Figure S2. Absorption (left) and normalized emission spectra (right) of α -NN (10 μ M) in various solvents at 25 $^{\circ}$ C. $\lambda_{\text{ex}} = 360$ nm.

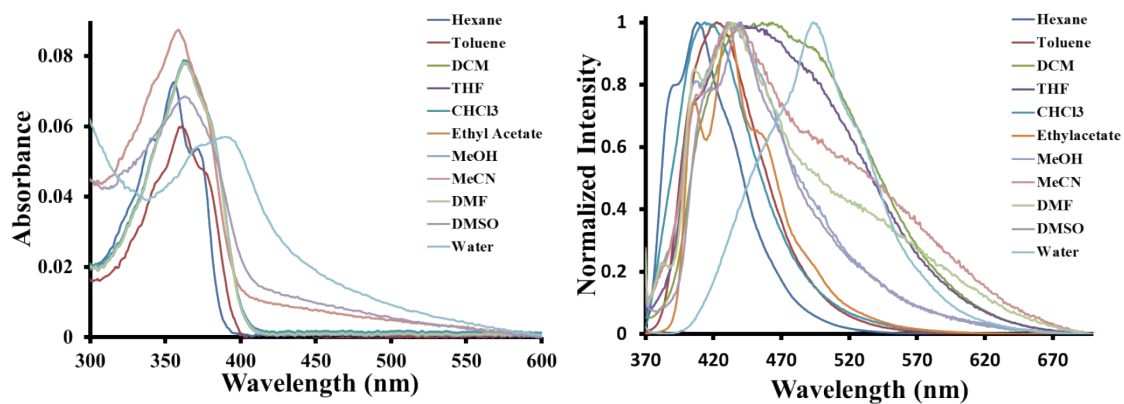


Figure S3. Absorption (left) and normalized emission spectra (right) of β -NN (10 μ M) in various solvents at 25 $^{\circ}$ C. $\lambda_{\text{ex}} = 360$ nm.

3. Study of AIEE Properties

Table S2. Photophysical properties of **α -NQ**, **α -NN** and **β -NN** various f_w (0%-99%) in DMF at 100 μ M concentration.

Compound	f_w in DMF	$\lambda_{\text{abs. max}}$ [nm]	ϵ^a [M ⁻¹ cm ⁻¹]	$\lambda_{\text{em. max}}^b$ [nm]	Stokes shift $\Delta\lambda/\text{nm}$	Φ_{FL} [%] ^c
α-NQ	0%	363	12844	437	74	1.45
	10%	364	14078	442	78	1.15
	20%	365	13372	443	78	0.99
	30%	366	13011	443	77	0.85
	40%	368	13211	445	77	0.59
	50%	368	10905	445	77	0.55
	60%	367	13516	450	83	1.64
	70%	363	10247	453	90	4.71
	80%	389	12251	493	104	4.77
	90%	389	12250	502	113	5.17
	99%	389	15071	509	120	6.89
α-NN	0%	361	11462	434	73	0.24
	10%	363	10923	446	83	0.16
	20%	364	10999	432	68	0.17
	30%	365	11139	427	62	0.19
	40%	366	11038	430	64	0.29
	50%	369	11354	482	113	3.50
	60%	388	12405	482	94	6.59
	70%	388	13750	481	93	5.95
	80%	387	13134	482	95	5.99
	90%	389	14217	482	93	4.71
	99%	389	13512	481	92	3.92
β-NN	0%	362	13125	435	73	0.06
	10%	363	12851	435	72	0.04
	20%	365	12221	439	74	0.04

30%	366	13252	440	74	0.03
40%	368	11566	457	89	0.11
50%	373	13184	495	122	3.32
60%	391	13255	493	102	5.07
70%	390	14238	494	104	4.77
80%	389	14280	494	105	4.07
90%	390	14628	495	105	3.34
99%	390	14629	494	104	2.79

^aMeasured at each absorption maximum. ^bExcited at 360 nm for all compounds. ^cQuantum yields were calculated by using quinine sulfate (0.1 M H₂SO₄, $\lambda_{\text{ex}}=350$ nm, $\Phi_{\text{FL}} = 57.7\%$) solution as reference together with the following formula: $\Phi_{\text{FL}} = \Phi_{\text{FL}}(I/I_{\text{R}})(A_{\text{R}}/A)(\eta^2/\eta_{\text{R}}^2)$, where Φ = quantum yield, I = Intensity of emission, A = absorbance at λ_{ex} , η = refractive index of solvent, R = reference. (100 μM)

Absorption and emission spectra of α -NQ, α -NN and β -NN in DMF at different water fraction

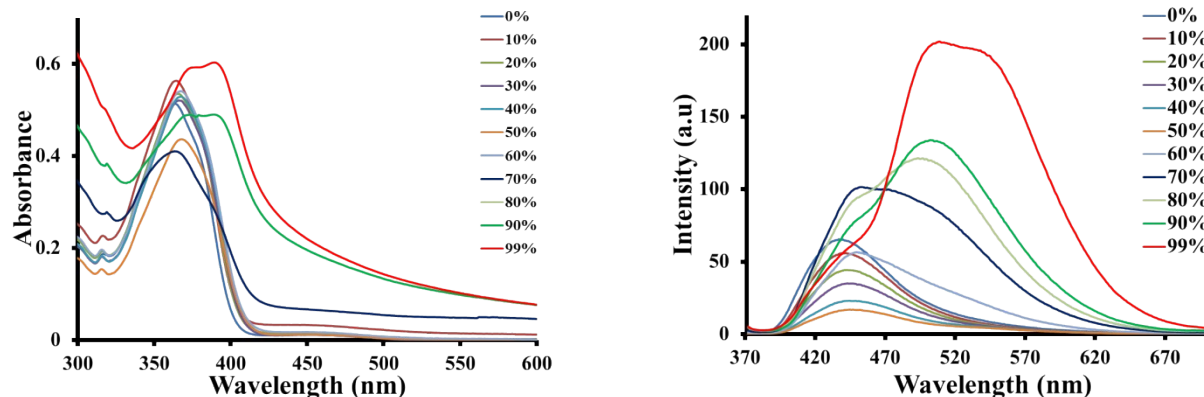


Figure S4. Absorption (left) and emission spectra (right) of α -NQ (100 μM) in DMF-Water mixtures with different volume fraction of water at 25 $^{\circ}\text{C}$. $\lambda_{\text{ex}} = 360$ nm.

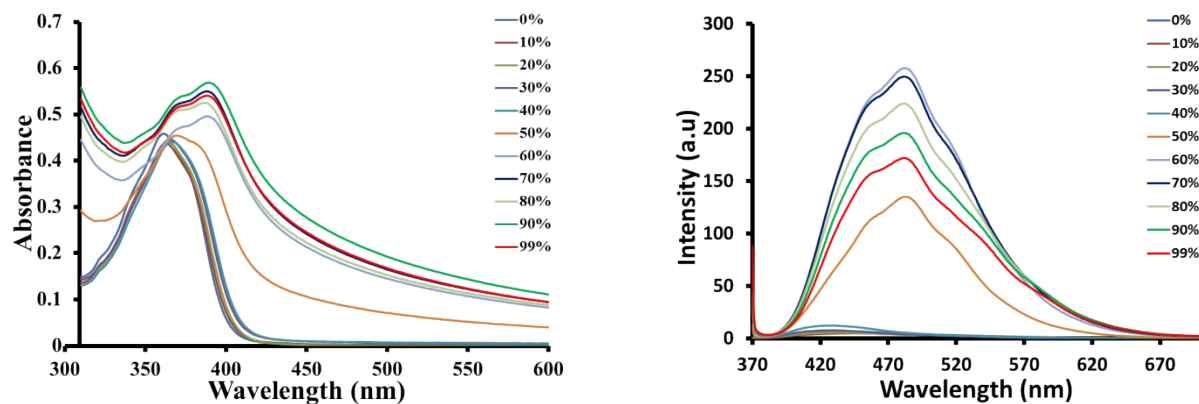


Figure S5. Absorption (left) and emission spectra (right) of α -NN (100 μ M) in DMF-Water mixtures with different volume fraction of water at 25 $^{\circ}$ C. $\lambda_{\text{ex}} = 360$ nm.

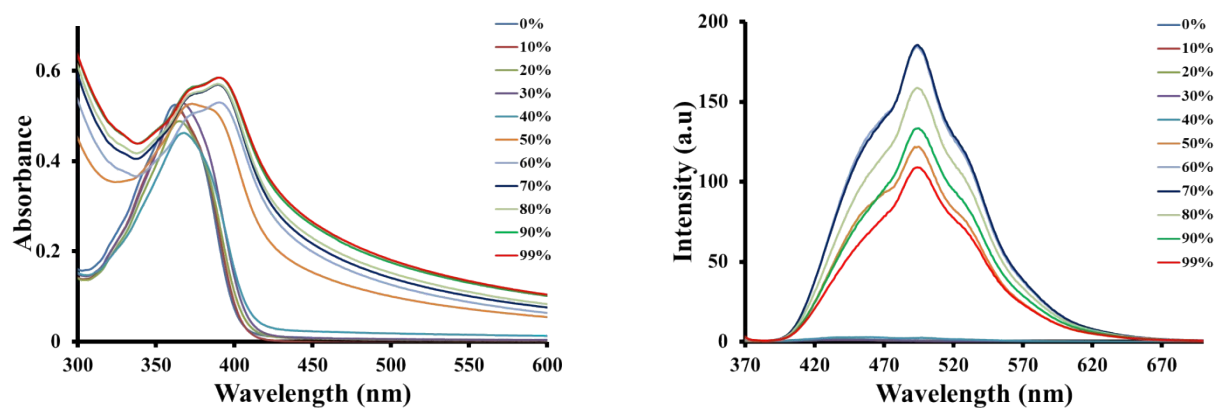


Figure S6. Absorption (left) and emission spectra (right) of β -NN (100 μ M) in DMF-Water mixtures with different volume fraction of water at 25 $^{\circ}$ C. $\lambda_{\text{ex}} = 360$ nm.

4. Time-Resolved Photoluminescence Study

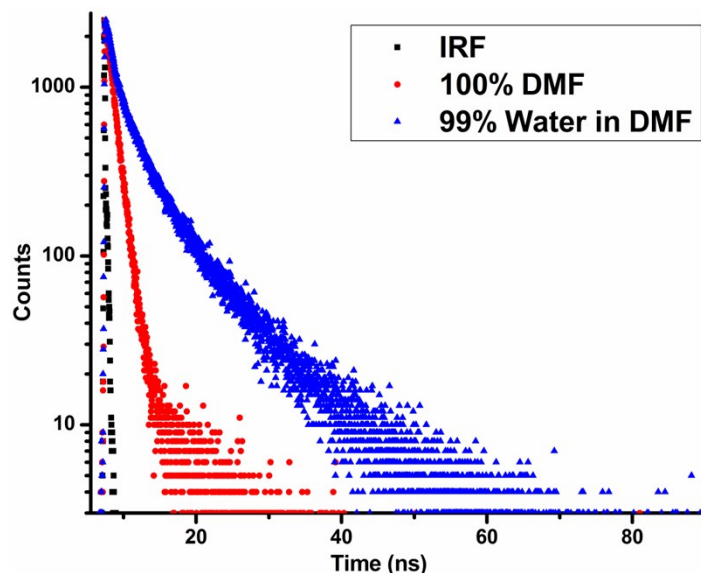


Figure S7. Time-resolved photoluminescence decay profiles of α -NQ (100 μ M) in DMF (red) for emission at 430 nm and in 99% Water-1% DMF mixture (blue) for emission at 545 nm. Mono-exponential decay with average lifetime of 0.144 ns in DMF and bi-exponential decay with average lifetime of 3.257 ns in 99% Water-1% DMF mixture. ($\lambda_{\text{ex}} = 375$ nm)

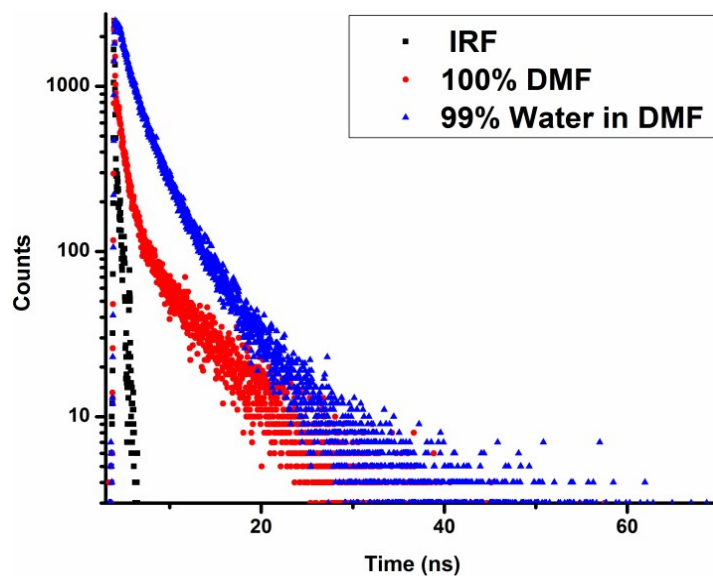


Figure S8. Time-resolved photoluminescence decay profiles of α -NN (100 μ M) in DMF (red) for emission at 430 nm and in 99% Water-1% DMF mixture (blue) for emission at 500 nm. Bi-exponential decays with average lifetimes of 2.606 ns in DMF and 3.459 ns in 99% Water-1% DMF mixture. ($\lambda_{\text{ex}} = 375$ nm)

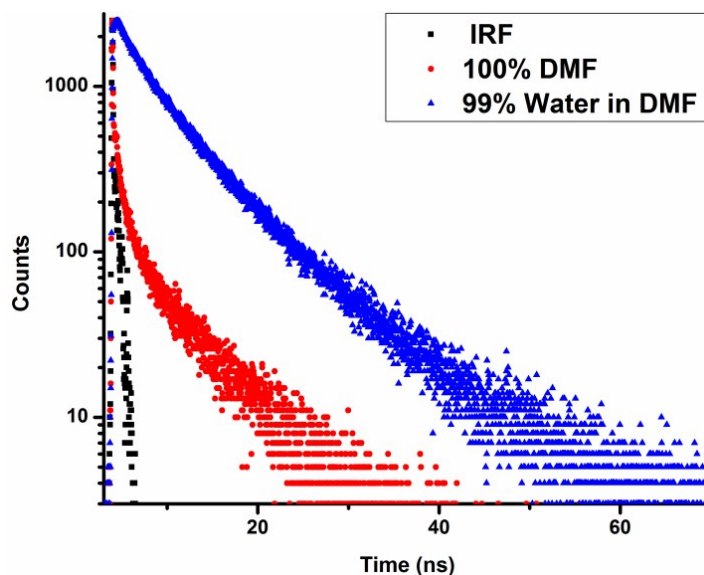


Figure S9. Time-resolved photoluminescence decay profiles of β -NN (100 μ M) in DMF (red) for emission at 430 nm and in 99% Water-1% DMF mixture (blue) for emission at 500 nm. Bi-exponential decays with average lifetimes of 3.328 ns in DMF and 5.275 ns in 99% Water-1% DMF mixture. ($\lambda_{\text{ex}} = 375$ nm)

Table S3. Time-Resolved Photoluminescence data of α -NQ, α -NN and β -NN in DMF and 99% Water in DMF (100 μ M).

Compound	Water (vol		τ_1 /ns (a_1)	τ_2 /ns (a_2)	χ^2	$\langle\tau\rangle$ ns	$k_F = \Phi_F/\tau$
	%)	in DMF					
α -NQ	0		1.079 (96.31)	5.691 (3.689)	0.972	1.249	1.1×10^7
	99		1.566 (52.55)	7.249 (47.54)	1.141	4.269	1.6×10^7
α -NN	0		1.167 (61.92)	4.945 (38.08)	0.998	2.606	7.6×10^5
	99		0.562 (45.78)	5.905 (54.22)	0.998	3.459	1.1×10^7
β -NN	0		0.556 (50.02)	6.102 (49.98)	0.951	3.328	1.8×10^5
	99		0.960 (45.41)	8.864 (54.59)	0.951	5.275	5.3×10^6

5. DLS Studies of Aggregates of α -NQ, α -NN and β -NN

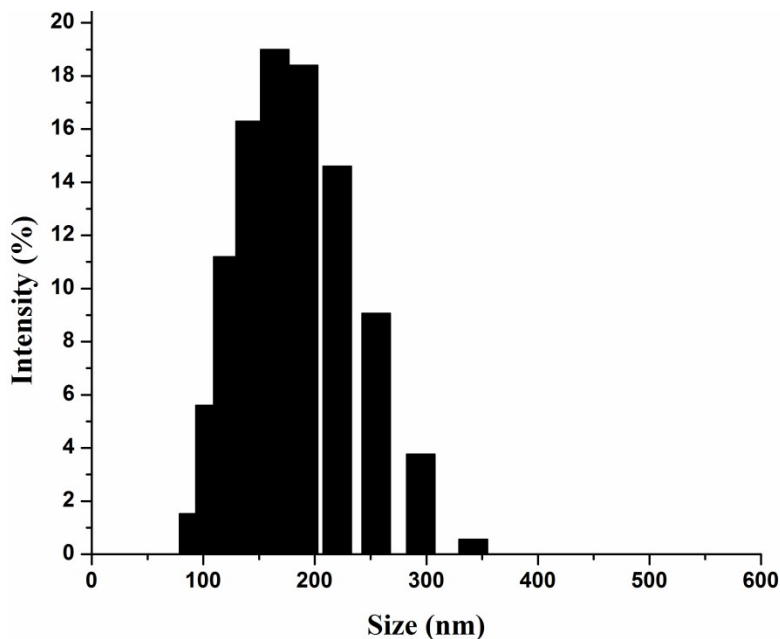


Figure S10. Size distribution by DLS of α -NQ aggregate (100 μ M) in 99% Water-1% DMF mixture solution at 25 $^{\circ}$ C. (Z_{ave} = 175.5 d.nm)

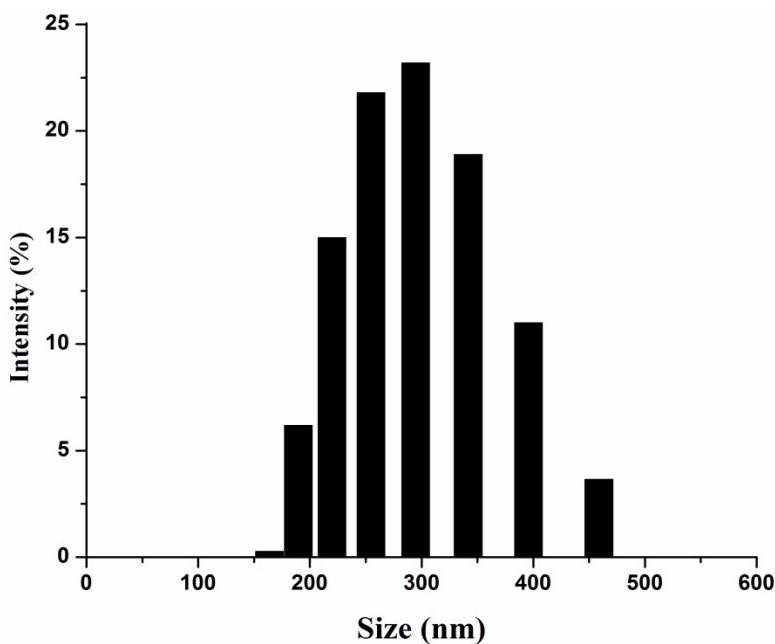


Figure S11. Size distribution by DLS of α -NN aggregate (100 μ M) in 99% Water-1% DMF mixture solution at 25 $^{\circ}$ C. (Z_{ave} = 280.9 d.nm)

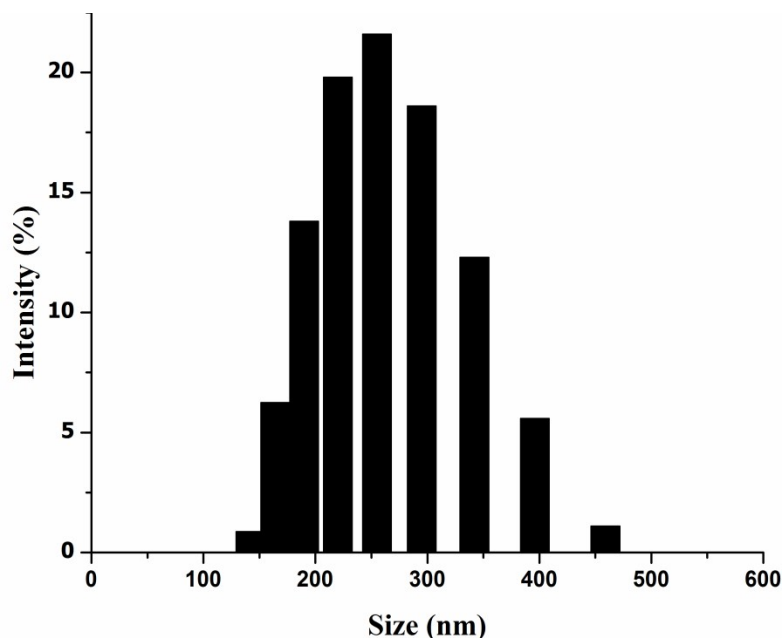


Figure S12. Size distribution by DLS of β -NN aggregate (100 μ M) in 99% Water-1% DMF mixture solution at 25 $^{\circ}$ C. (Z_{ave} = 246.2 d.nm)

6. X-ray Structures and data of α -NQ and β -NN

Concentrated solutions of α -NQ, α -NN and β -NN in DMF were prepared by heating at 60 $^{\circ}$ C and then they were filtered off to leave behind the undissolved compound. After about a week, block shaped crystals for α -NQ and β -NN suitable for X-ray structure analysis were obtained. However, several attempts to obtain crystals for α -NN in various solvents and their mixture failed and very fine niddle shaped crystal of less than 100 μ M in width were produced that were not suitable for single crystal analysis (Fig. S17, ESI †).

Table S4. Single Crystal Data and Parameters for crystals of α -NQ (**3**) and β -NN (**1**)

Compound Code	3	1
CCDC	1452816	1454751
Empirical Formula	C27 H24 N2 O3	C28 H25 N1 O3
Formula Weight	424.48	423.49
Temperature	293(2) K	293(2) K
Wavelength	0.71073 Å	0.71073 Å
Crystal System	monoclinic	monoclinic

Space Group	P 21/c	P 21/n
Unit Cell Dimension	a = 10.2888(5) Å	a = 8.2646(5) Å
	$\alpha = 90^\circ$	$\alpha = 90^\circ$
	b = 16.2882(10) Å	b = 14.0049(12) Å
	$\beta = 91.491(5)^\circ$	$\beta = 98.030(6)^\circ$
	c = 13.2480(6) Å	c = 19.1830(12) Å
	$\gamma = 90^\circ$	$\gamma = 90^\circ$
Volume	2219.4(2) Å ³	2198.6(2) Å ³
Z	4	4
Density (Calculated)	1.270 Mg/m ³	1.285 Mg/m ³
Absorption coefficient	0.083 mm ⁻¹	0.083 mm ⁻¹
F (000)	736	7900
Crystal Size		
Theta range for data collection	3.191 to 28.712°	3.171 to 28.512°
Index Range	-8 ≤ h ≤ 13, -21 ≤ k ≤ 21, -17 ≤ l ≤ 17	-10 ≤ h ≤ 11, -- 17 ≤ k ≤ 18, -25 ≤ l ≤ 10
Reflections Collected	9684	10495
Independent Reflection	2549 [R(int) = 0.0248]	3119 [R(int) = 0.00380]
Refinement method	SHELXL-2014/7 (Sheldrick, 2014)	SHELXL-2014/7 (Sheldrick, 2014)
Goodness-of-fit on F ²	1.062	0.962
Final R indices [I > 2σ(I)]	R1 = 0.0799, ωR2 = 0.2671	R1 = 0.0635, ωR2 = 0.2338
R indices (all data)	R1 = 0.1447, ωR2 = 0.3323	R1 = 0.0999, ωR2 = 0.2911

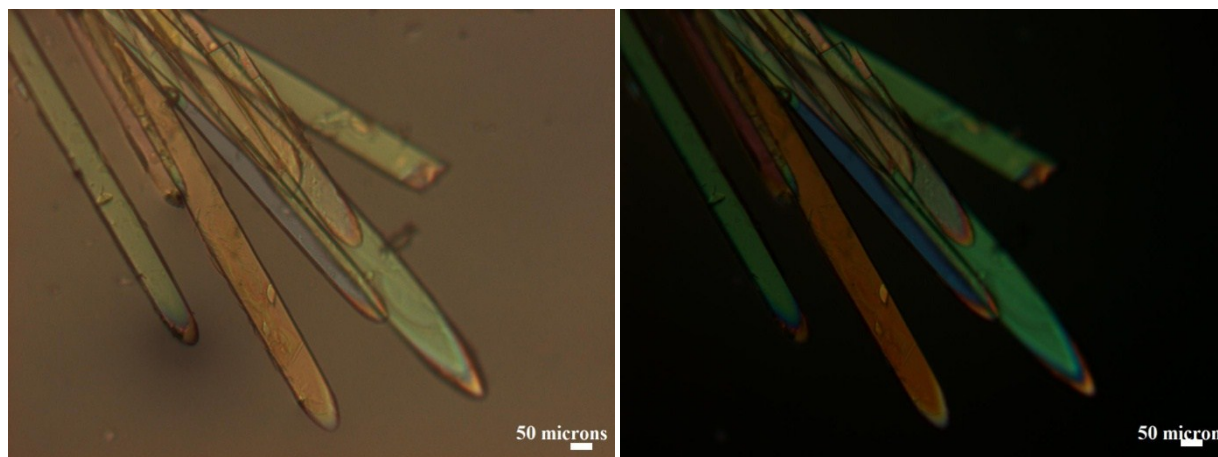


Figure S13. Polarized Optical Microscopic images of very fine needle like crystals of α -NN with (left) and without (right) the use of polarizing light. After a number of attempts, we able to get the very fine crystal of α -NN from 1:1 (V/V) DMF/DMSO mixture. The crystals are of very low strength and $\sim 100 \mu\text{M}$ in width which are quite incompatible for X-ray crystal analysis.

7. Computational Methods

Ground state geometric optimizations were done by density functional theory (DFT) with the B3LYP functional³ as implemented in Gaussian 03 software package⁴ using the 6-31G basis set. Absolute energies are given in hartrees or eV without additional corrections. Dipole moments were calculated by single point calculations (B3LYP/6-31+G(d)) using the optimized structures.

Cartesian Coordinates for α -NQ:

Atoms	X	Y	Z
C	2.54556	1.35775	-0.77298
C	1.19861	1.83222	-0.38649
C	0.19048	0.90672	-0.02806
C	0.45354	-0.48348	-0.03386
C	1.78134	-0.99998	-0.4124
C	0.93813	3.18924	-0.38068
C	-1.09901	1.39032	0.33798
C	-1.34281	2.78569	0.33193
C	-0.33898	3.6674	-0.02096
C	-2.09778	0.4378	0.6919

C	-1.82225	-0.9157	0.68512
C	-0.54496	-1.37262	0.31922
H	-0.31469	-2.43078	0.30897
H	-2.59421	-1.62197	0.9577
H	1.73784	3.86367	-0.66093
H	-0.53134	4.73323	-0.02534
N	2.74263	-0.03211	-0.77008
O	3.46749	2.12955	-1.08864
O	2.0564	-2.21159	-0.42951
O	-3.31432	0.98267	1.09698
C	-4.48714	0.21113	1.13164
C	-5.03441	-0.31333	-0.07502
C	-5.12395	0.03146	2.33576
C	-6.26651	-1.03537	0.00273
C	-6.34793	-0.67735	2.39741
H	-4.67873	0.44832	3.22913
C	-4.90337	-0.60203	-2.36613
C	-6.79336	-1.54686	-1.21463
C	-6.90947	-1.20583	1.25755
H	-6.83494	-0.80369	3.35649
C	-6.11764	-1.33355	-2.39363
H	-4.35975	-0.42469	-3.28805
H	-7.72576	-2.10021	-1.1952
H	-7.84465	-1.75259	1.30153
H	-6.49555	-1.7118	-3.33477
N	-4.37403	-0.10627	-1.25449
C	4.09472	-0.51756	-1.15757
C	5.10582	-0.37369	-0.00359
H	4.4215	0.0794	-2.01168
H	3.97407	-1.56464	-1.43572
C	6.50438	-0.87604	-0.42157

H	5.16011	0.68436	0.27394
H	4.74692	-0.94698	0.85961
H	6.44056	-1.93235	-0.71814
H	6.84434	-0.30929	-1.29963
C	7.54657	-0.72797	0.70871
C	8.95164	-1.21354	0.28993
H	7.21351	-1.29934	1.58628
H	7.60374	0.3272	1.01001
C	9.98632	-1.05657	1.425
H	8.89274	-2.26808	-0.01104
H	9.28042	-0.64351	-0.5892
H	10.97561	-1.4068	1.10988
H	10.07346	-0.00495	1.72252
H	9.68191	-1.63523	2.30514
H	-2.32901	3.13483	0.60605

Cartesian Coordinates for α -NN:

Atoms	X	Y	Z
C	2.54556	1.35775	-0.77298
C	1.19861	1.83222	-0.38649
C	0.19048	0.90672	-0.02806
C	0.45354	-0.48348	-0.03386
C	1.78134	-0.99998	-0.4124
C	0.93813	3.18924	-0.38068
C	-1.09901	1.39032	0.33798
C	-1.34281	2.78569	0.33193
C	-0.33898	3.6674	-0.02096
C	-2.09778	0.4378	0.6919
C	-1.82225	-0.9157	0.68512
C	-0.54496	-1.37262	0.31922
H	-0.31469	-2.43078	0.30897

H	-2.59421	-1.62197	0.9577
H	1.73784	3.86367	-0.66093
H	-0.53134	4.73323	-0.02534
N	2.74263	-0.03211	-0.77008
O	3.46749	2.12955	-1.08864
O	2.0564	-2.21159	-0.42951
O	-3.31432	0.98267	1.09698
C	-4.48714	0.21113	1.13164
C	-5.03441	-0.31333	-0.07502
C	-5.12395	0.03146	2.33576
C	-6.26651	-1.03537	0.00273
C	-6.34793	-0.67735	2.39741
H	-4.67873	0.44832	3.22913
C	-4.90337	-0.60203	-2.36613
C	-6.79336	-1.54686	-1.21463
C	-6.90947	-1.20583	1.25755
H	-6.83494	-0.80369	3.35649
C	-6.11764	-1.33355	-2.39363
H	-4.35975	-0.42469	-3.28805
H	-7.72576	-2.10021	-1.1952
H	-7.84465	-1.75259	1.30153
H	-6.49555	-1.7118	-3.33477
C	4.09472	-0.51756	-1.15757
C	5.10582	-0.37369	-0.00359
H	4.4215	0.0794	-2.01168
H	3.97407	-1.56464	-1.43572
C	6.50438	-0.87604	-0.42157
H	5.16011	0.68436	0.27394
H	4.74692	-0.94698	0.85961
H	6.44056	-1.93235	-0.71814
H	6.84434	-0.30929	-1.29963

C	7.54657	-0.72797	0.70871
C	8.95164	-1.21354	0.28993
H	7.21351	-1.29934	1.58628
H	7.60374	0.3272	1.01001
C	9.98632	-1.05657	1.425
H	8.89274	-2.26808	-0.01104
H	9.28042	-0.64351	-0.5892
H	10.97561	-1.40681	1.10988
H	10.07346	-0.00495	1.72252
H	9.68191	-1.63523	2.30514
H	-2.32901	3.13483	0.60605
C	-4.37403	-0.10627	-1.25449
H	-3.45491	0.44094	-1.28051

Cartesian Coordinates for β -NN:

Atoms	X	Y	Z
C	2.54556	1.35775	-0.77298
C	1.19861	1.83222	-0.38649
C	0.19048	0.90672	-0.02806
C	0.45354	-0.48348	-0.03386
C	1.78134	-0.99998	-0.4124
C	0.93813	3.18924	-0.38068
C	-1.09901	1.39032	0.33798
C	-1.34281	2.78569	0.33193
C	-0.33898	3.6674	-0.02096
C	-2.09778	0.4378	0.6919
C	-1.82225	-0.9157	0.68512
C	-0.54496	-1.37262	0.31922
H	-0.31469	-2.43078	0.30897
H	-2.59421	-1.62197	0.9577
H	1.73784	3.86367	-0.66093

H	-0.53134	4.73323	-0.02534
N	2.74263	-0.03211	-0.77008
O	3.46749	2.12955	-1.08864
O	2.0564	-2.21159	-0.42951
O	-3.31432	0.98267	1.09698
C	4.09472	-0.51756	-1.15757
C	5.10582	-0.37369	-0.00359
H	4.4215	0.0794	-2.01168
H	3.97407	-1.56464	-1.43572
C	6.50438	-0.87604	-0.42157
H	5.16011	0.68436	0.27394
H	4.74692	-0.94698	0.85961
H	6.44056	-1.93235	-0.71814
H	6.84434	-0.30929	-1.29963
C	7.54657	-0.72797	0.70871
C	8.95164	-1.21354	0.28993
H	7.21351	-1.29934	1.58628
H	7.60374	0.3272	1.01001
C	9.98632	-1.05657	1.425
H	8.89274	-2.26808	-0.01104
H	9.28042	-0.64351	-0.5892
H	10.97561	-1.40681	1.10988
H	10.07346	-0.00495	1.72252
H	9.68191	-1.63523	2.30514
H	-2.32901	3.13483	0.60605
C	-3.07351	2.11388	1.93797
C	-4.15543	2.87438	2.40002
C	-1.77048	2.45432	2.29324
C	-3.90929	3.99574	3.23421
C	-1.51991	3.55328	3.11161
H	-0.92958	1.84846	1.92322

C	-5.00441	4.78505	3.71599
C	-2.57842	4.33539	3.59122
H	-0.48614	3.81218	3.38522
C	-4.75829	5.90641	4.55025
C	-2.36087	5.47869	4.43874
C	-3.39738	6.22569	4.89476
H	-1.32155	5.72608	4.70454
H	-3.2269	7.09949	5.54241
H	-5.15635	2.61266	2.12699
H	-6.00773	4.52875	3.44659
H	-5.56801	6.50268	4.91592

Calculated Dipole Moment

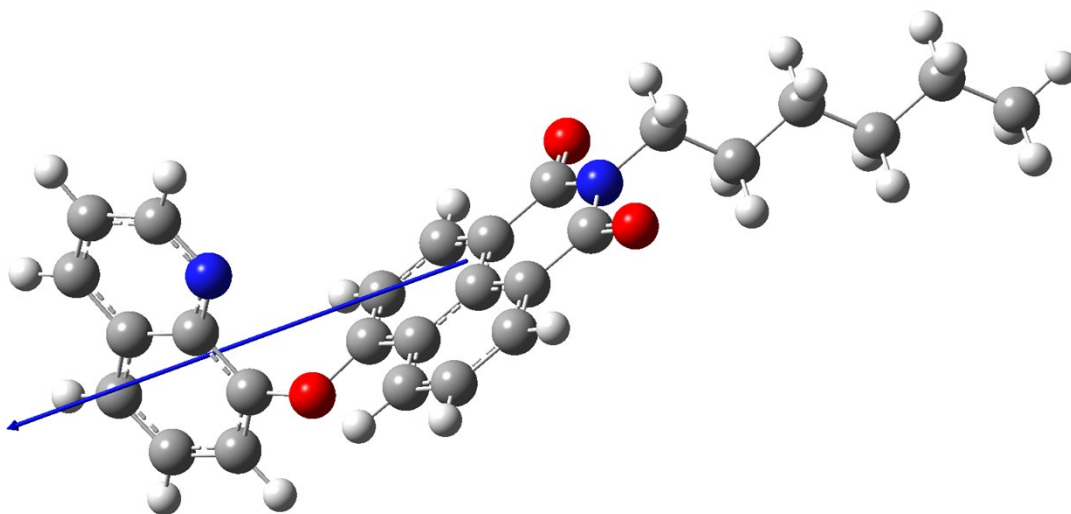


Figure S14: Dipole Moment of α -NQ is 7.8829 Debye

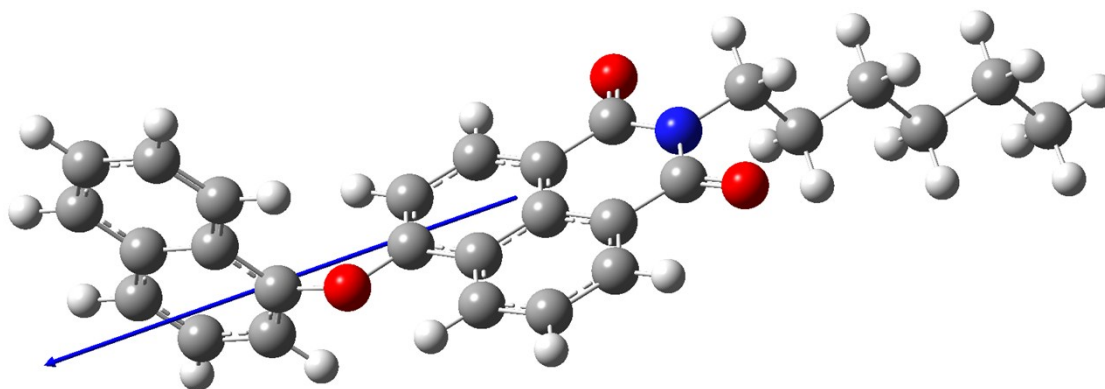


Figure S15: Dipole Moment of α -NN is 5.7126 Debye

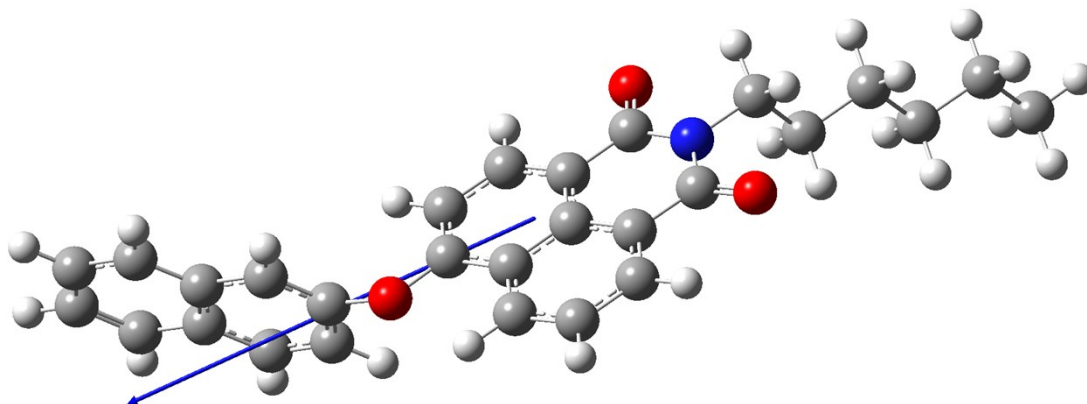


Figure S16: Dipole Moment of β -NN is 6.0270 Debye

8. AFM Images of aggregates of α -NQ, α -NN and β -NN

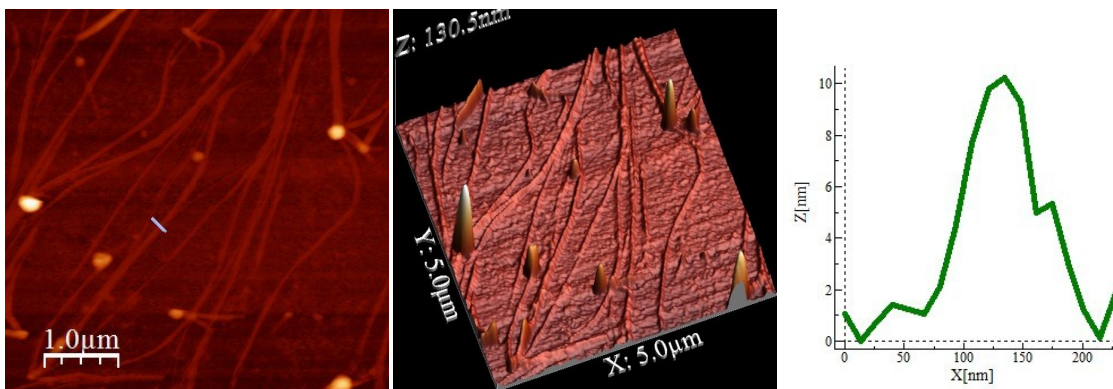


Figure S17. AFM images showing 2D, 3D and Height Profile diagram (left to right) of α -NQ formed from evaporation of 99.9% H₂O- 0.1% DMF mixture on glass slide at room temperature. (Concentration: 10 μ M)

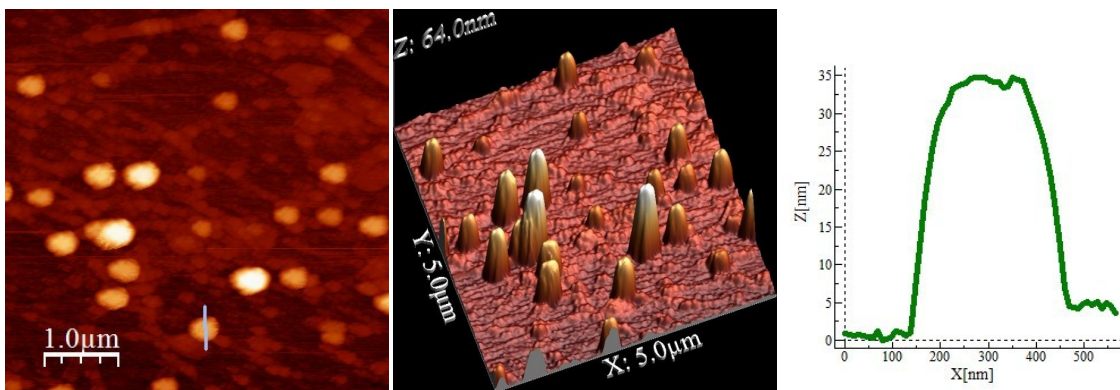


Figure S18. AFM images showing 2D, 3D and Height Profile diagram (left to right) of α -NN formed from evaporation of 99.9% H₂O- 0.1% DMF mixture on glass slide at room temperature. (Concentration: 10 μM)

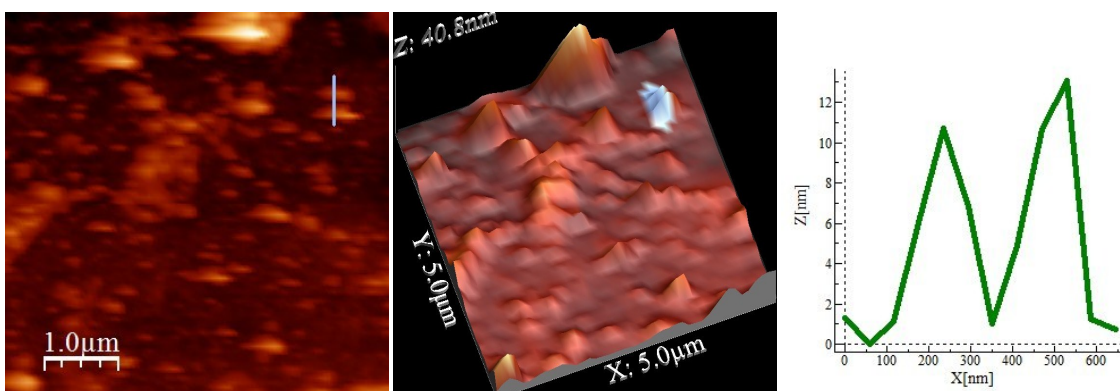


Figure S19. AFM images showing 2D, 3D and Height Profile diagram (left to right) of β -NN formed from evaporation of 99.9% H₂O- 0.1% DMF mixture on glass slide at room temperature. (Concentration: 10 μM)

9. FE-SEM and TEM Images of aggregates α -NQ

The morphology of the aggregates of α -NQ was determined by field effect scanning electron microscopy (FE-SEM). The FE-SEM images of the dried aggregates of α -NQ in 99.9% *fw* mixtures confirmed a 1D-network of nanoribbons of less than 100 nm in diameter with continuous one directional growth. Also the nanoribbons were analyzed by TEM imaging where their solid nature was confirmed.

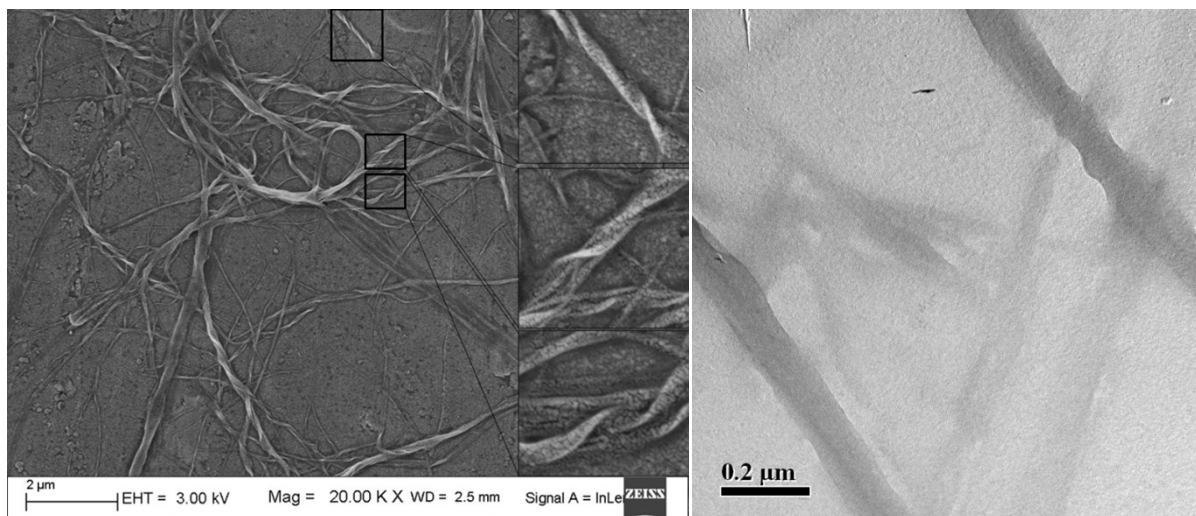


Figure S20. The magnified view of nanoribbons recorded by FE-SEM (left) and TEM (right) formed from evaporation of 99.9% H₂O-0.1% DMF mixture solution of α -NQ at room temperature. (Concentration: 10 μ M)

10. Sensing studies and calculations.

The monomer α -NQ (4.2 mg) stock solution was prepared at a concentration of 10 mM in 1 mL DMF. This was diluted to 20 μ M for each titration in a 1 mL cuvette. The stock solutions of metalloproteins and non-metalloproteins (ferritin concentration taken was 0.1 mM, rest were of 1mM) were introduced in portions and the fluorescence intensity changes were recorded at pH 7.4 at room temperature (excitation wavelength: 360 nm) in Tris-buffer.

Calculation of Detection Limit

For calculating detection limit, different samples of α -NQ (20 μ M) each containing Ferritin (0 nM, 10 nM, 20 nM, 30 nM and 40 nM) were prepared separately and fluorescence spectrum was then recorded for each sample by exciting at 360 nm. The detection limit plot for Ferritin was obtained by plotting change in the fluorescence intensity vs I_0/I of Ferritin. The curve shows a linear relationship and the correlation coefficient (R^2) via linear regression analysis was calculated to be 0.9966. The limit of detection (LOD) was then calculated using the equation $3\sigma/K$, where σ represents the standard deviation for the intensity of α -NQ in the absence of Ferritin and K symbolizes slope of the equation. The ferritin used was from horse spleen having molecular weight more than 5 lakhs.⁵

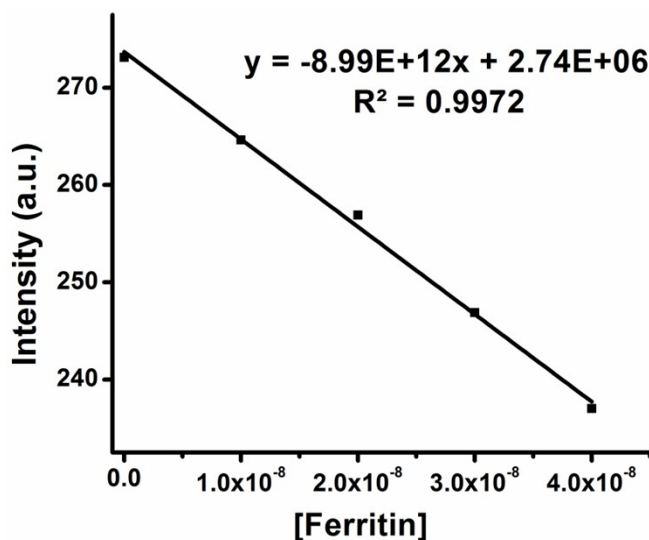


Fig. S21 Fluorescence response of α -NQ (20 μ M) taken in aqueous solution (at pH 7.4) as a function of Ferritin concentration.

$$\text{LOD} = 3 \times \text{S.D.} / k$$

$$\text{LOD} = 3 \times 2015.279 / 8.99 \times 10^{12}$$

$$= 67.25 \times 10^{-11} \text{ M} \quad (0.33 \text{ ng}/\mu\text{L})$$

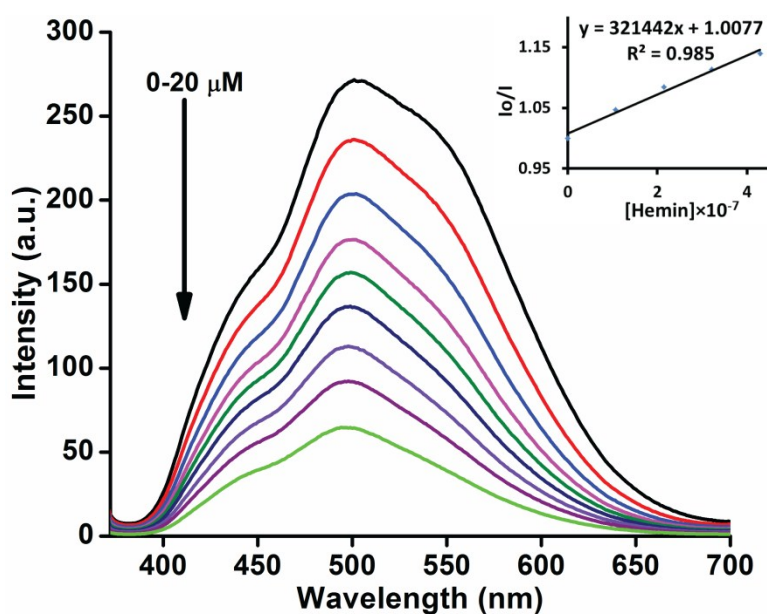


Figure S22. Effect of increasing concentration of Hemin on the fluorescence spectra of α -NQ (20 μ M at pH 7.4) at room temperature. Inset is the Stern–Volmer plots for the fluorescence quenching of α -NQ by hemin.

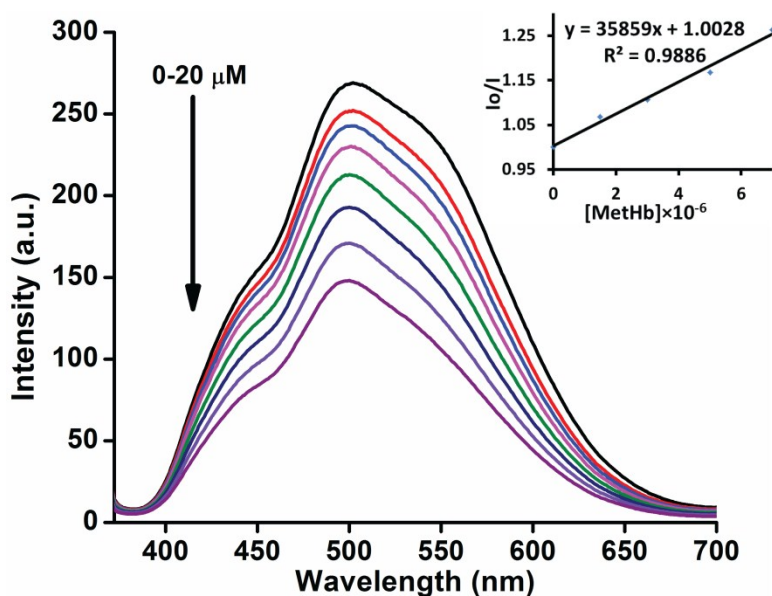


Figure S23. Effect of increasing concentration of MetHb on the fluorescence spectra of α -NQ (20 μ M at pH 7.4) at room temperature. Inset is the Stern–Volmer plots for the fluorescence quenching of α -NQ by MetHb.

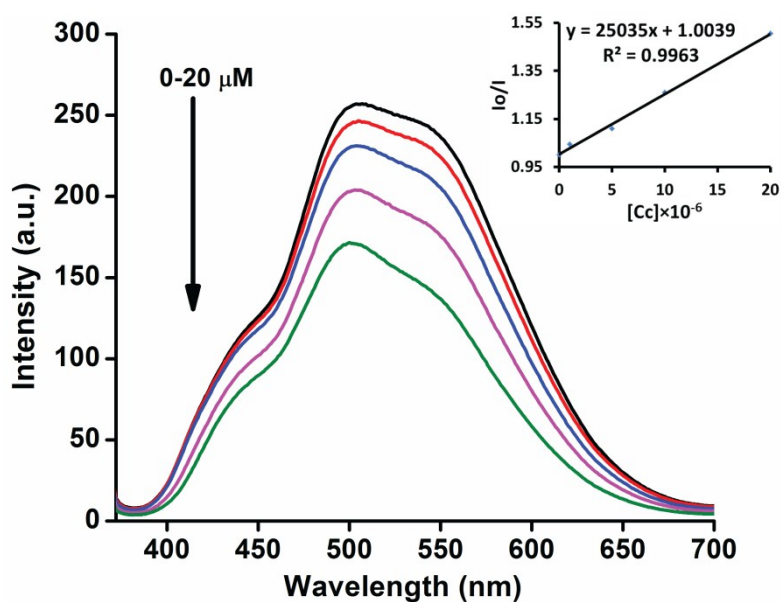


Figure S24. Effect of increasing concentration of Cc on the fluorescence spectra of α -NQ (20 μ M at pH 7.4) at room temperature. Inset is the Stern–Volmer plots for the fluorescence quenching of α -NQ by Cc.

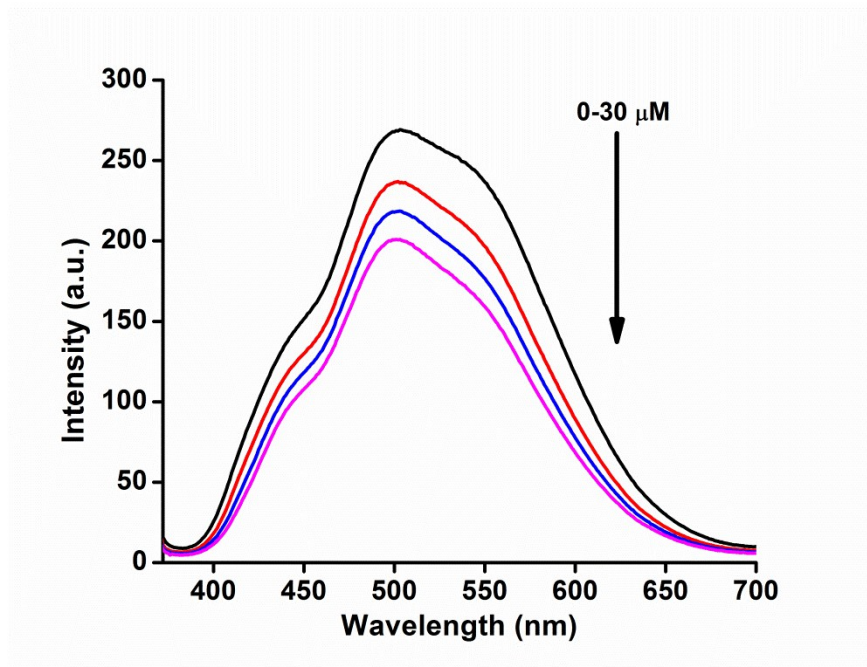


Figure S25. Effect of increasing concentration of Vit B₁₂ on the fluorescence spectra of α -NQ (20 μ M at pH 7.4) at room temperature.

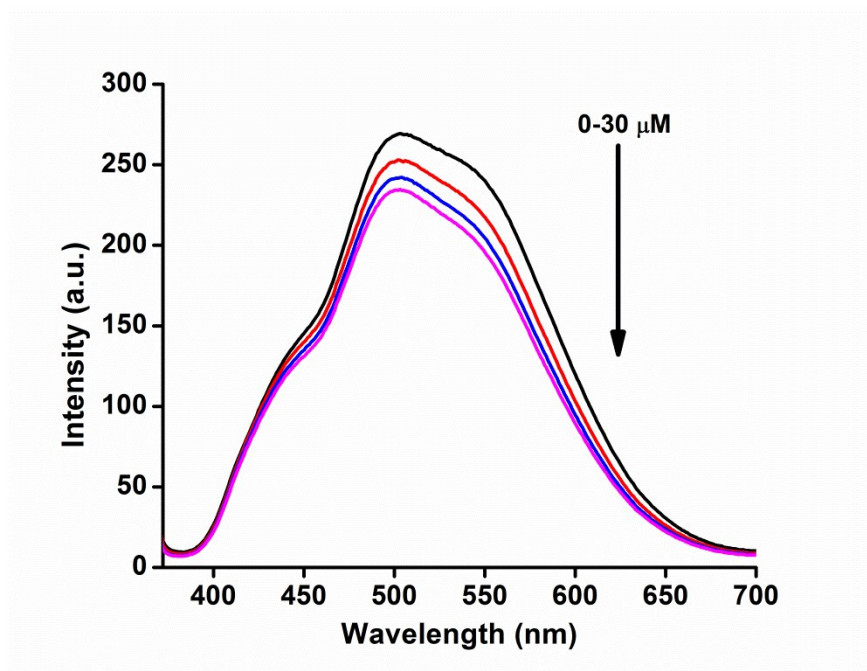


Figure S26. Effect of increasing concentration of Lysozyme on the fluorescence spectra of α -NQ (20 μ M at pH 7.4) at room temperature.

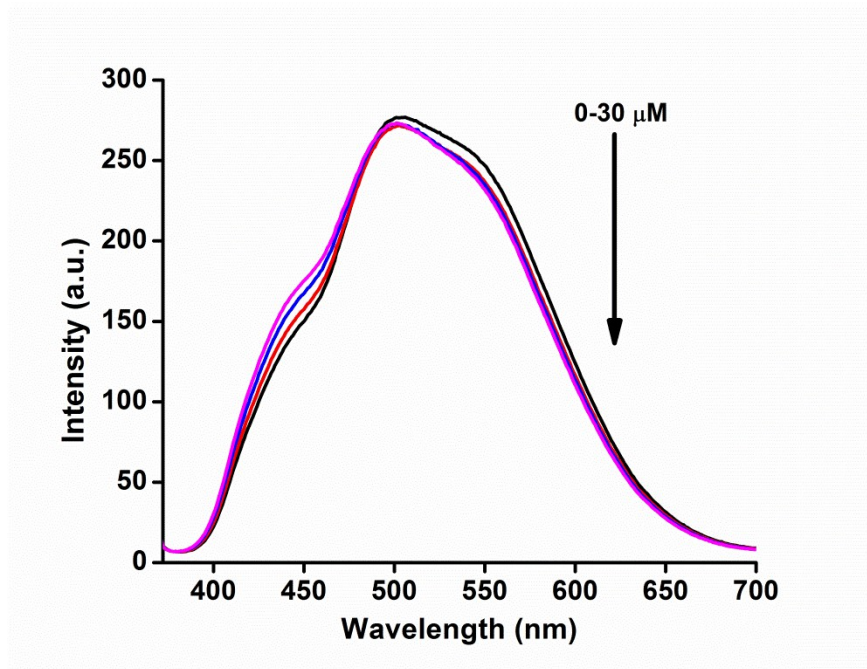


Figure S27. Effect of increasing concentration of BSA on the fluorescence spectra of α -NQ (20 μ M at pH 7.4) at room temperature.

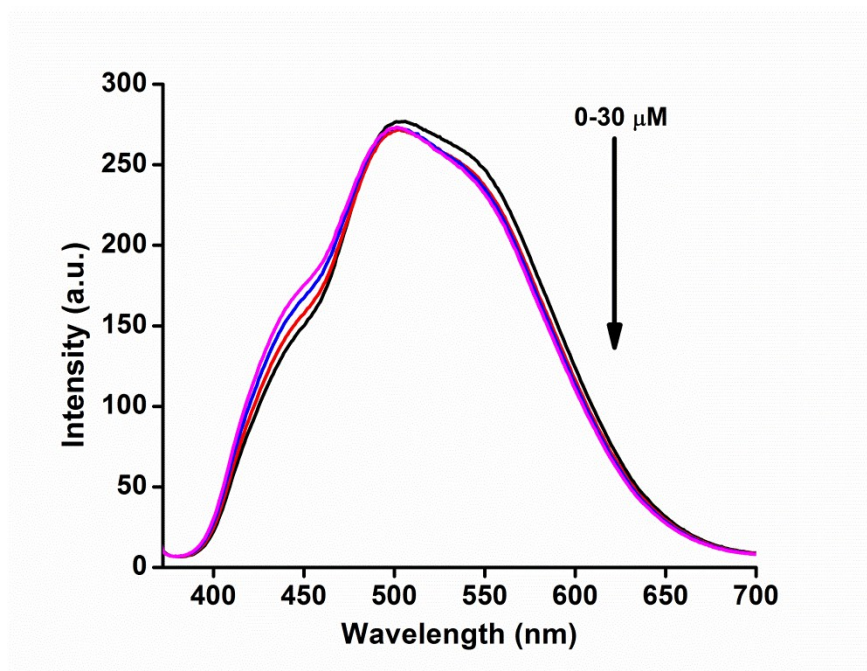


Figure S28. Effect of increasing concentration of Insuline on the fluorescence spectra of α -NQ (20 μ M at pH 7.4) at room temperature.

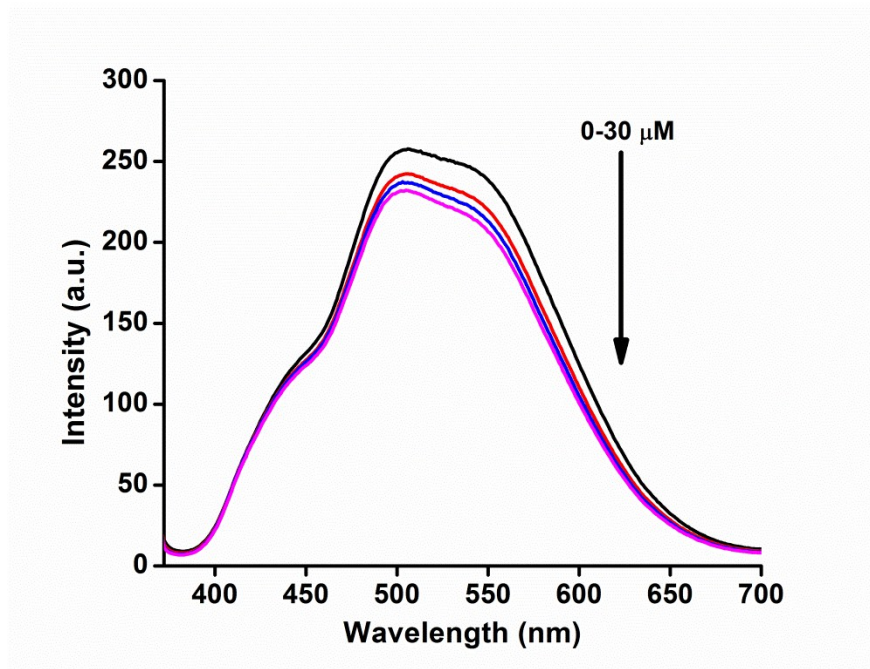


Figure S29. Effect of increasing concentration of RNase on the fluorescence spectra of α -NQ (20 μ M at pH 7.4) at room temperature.

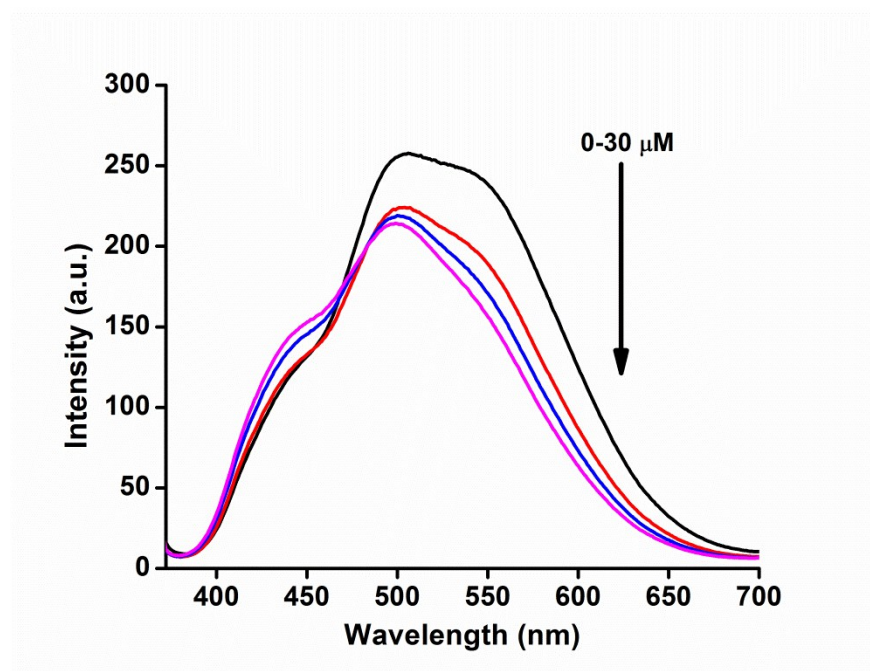


Figure S30. Effect of increasing concentration of Casein on the fluorescence spectra of α -NQ (20 μ M at pH 7.4) at room temperature.

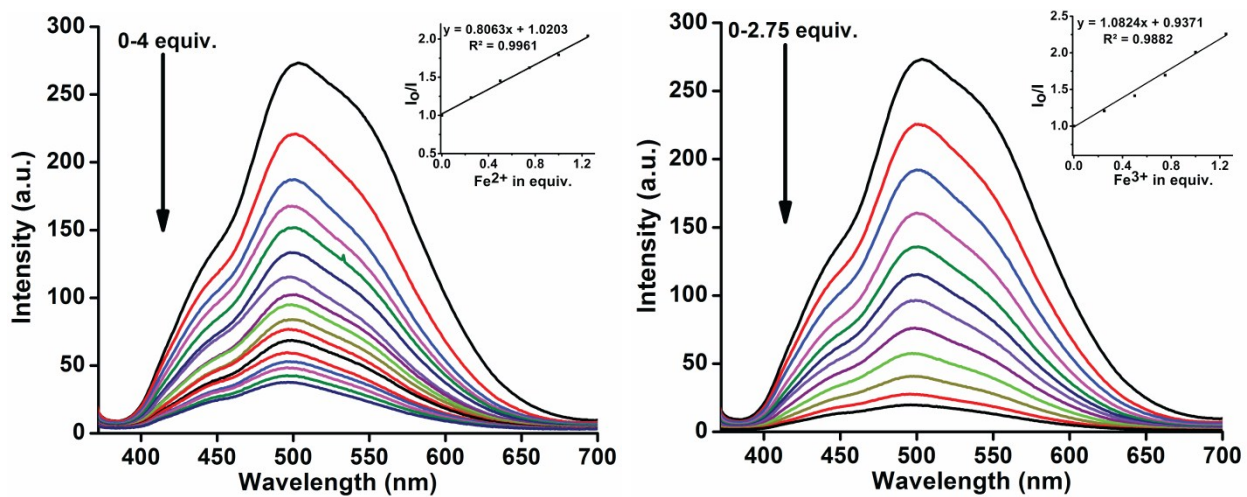
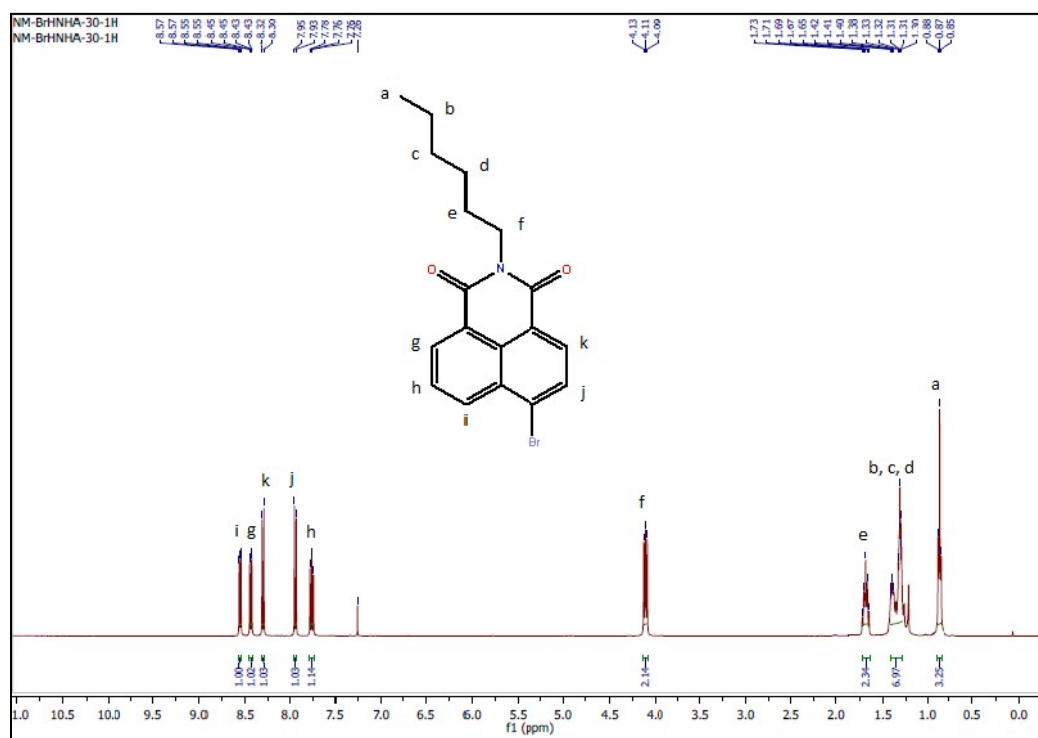
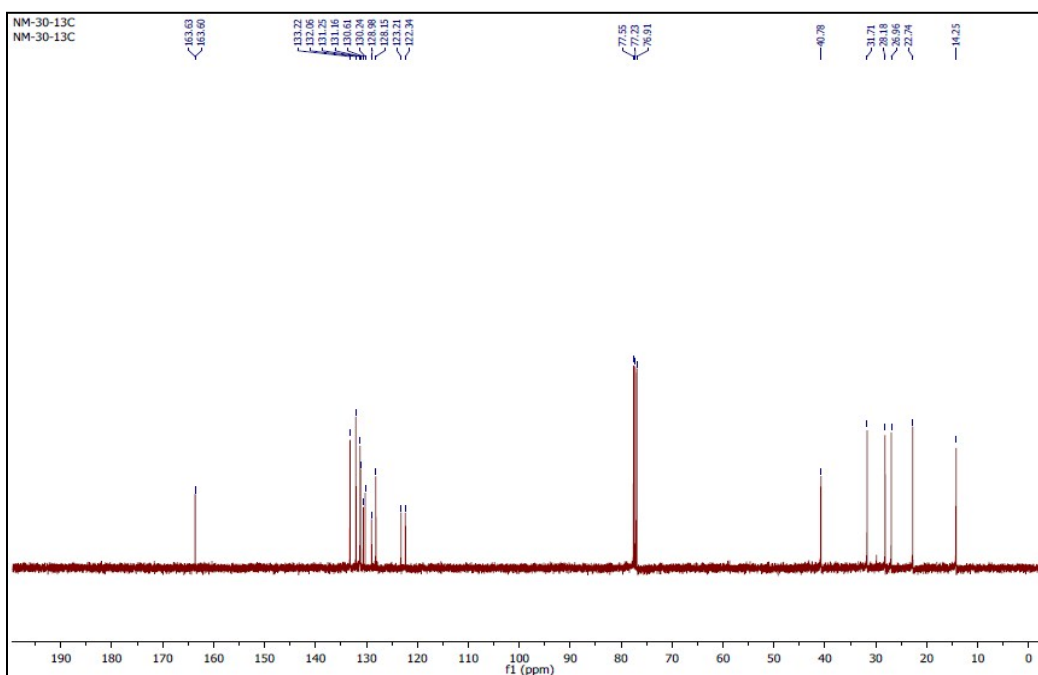


Figure S31. Fluorescence response of α -NQ (20 μM at pH 7.4) in presence of various concentrations of Fe^{2+} (left) and Fe^{3+} (right) at room temperature.

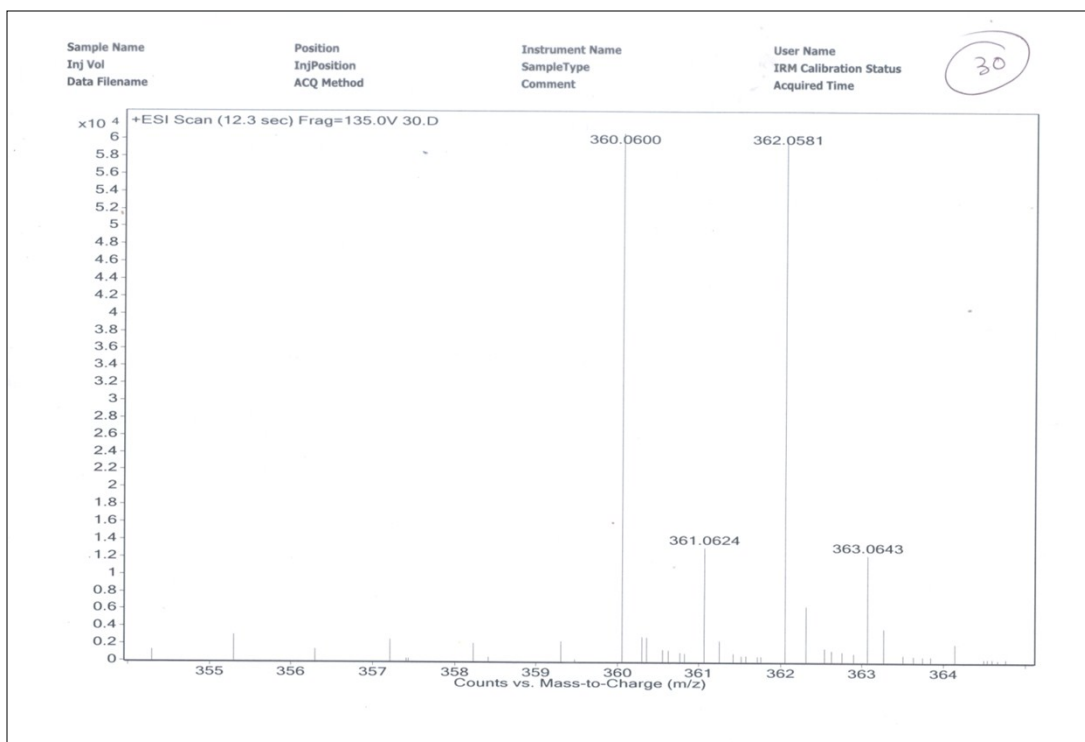
11. ¹H-NMR, ¹³C-NMR and Mass Spectra



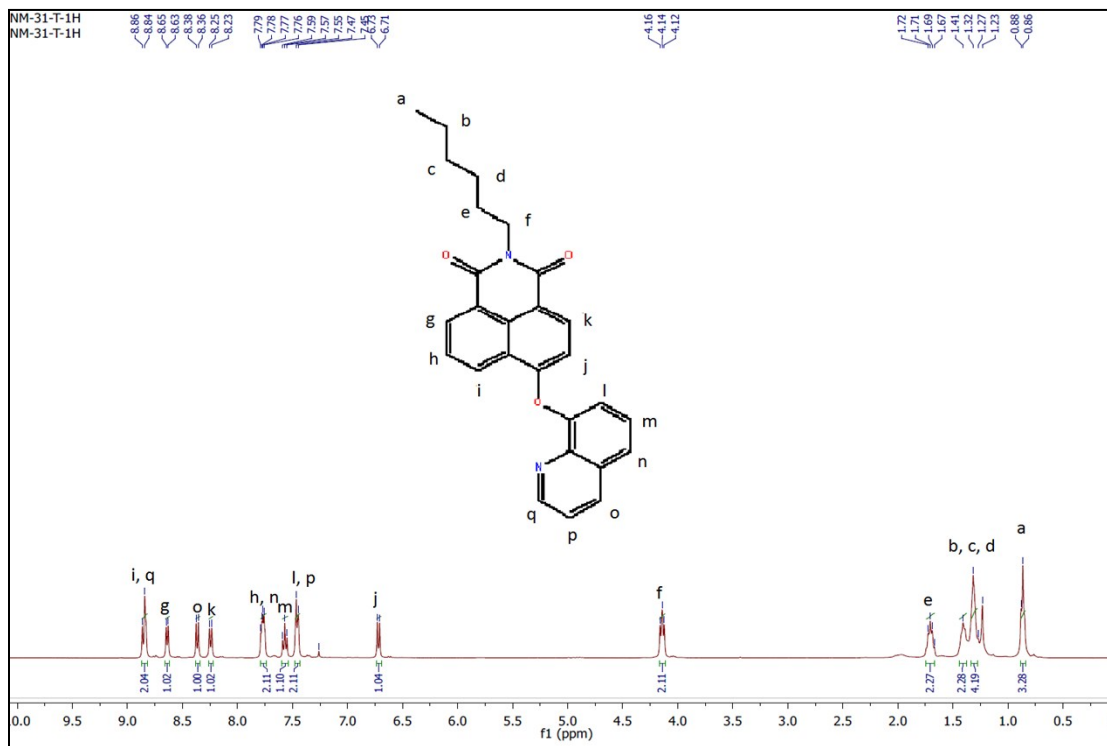
¹H NMR of 6N



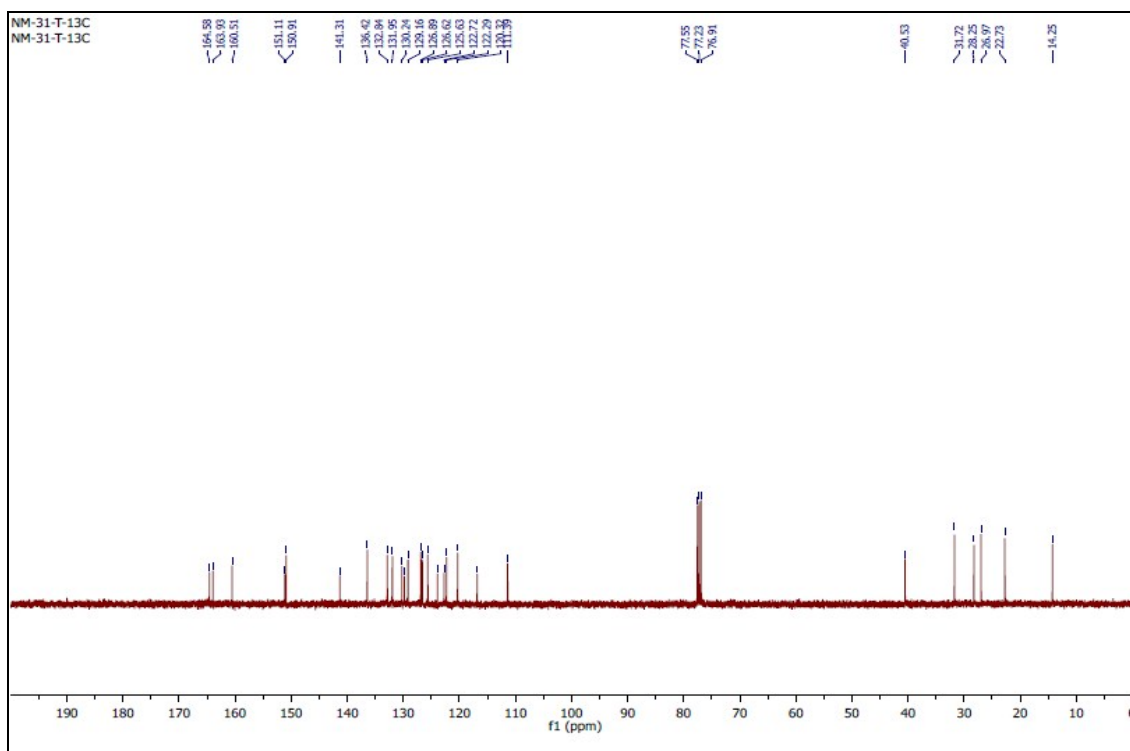
¹³C NMR of 6N



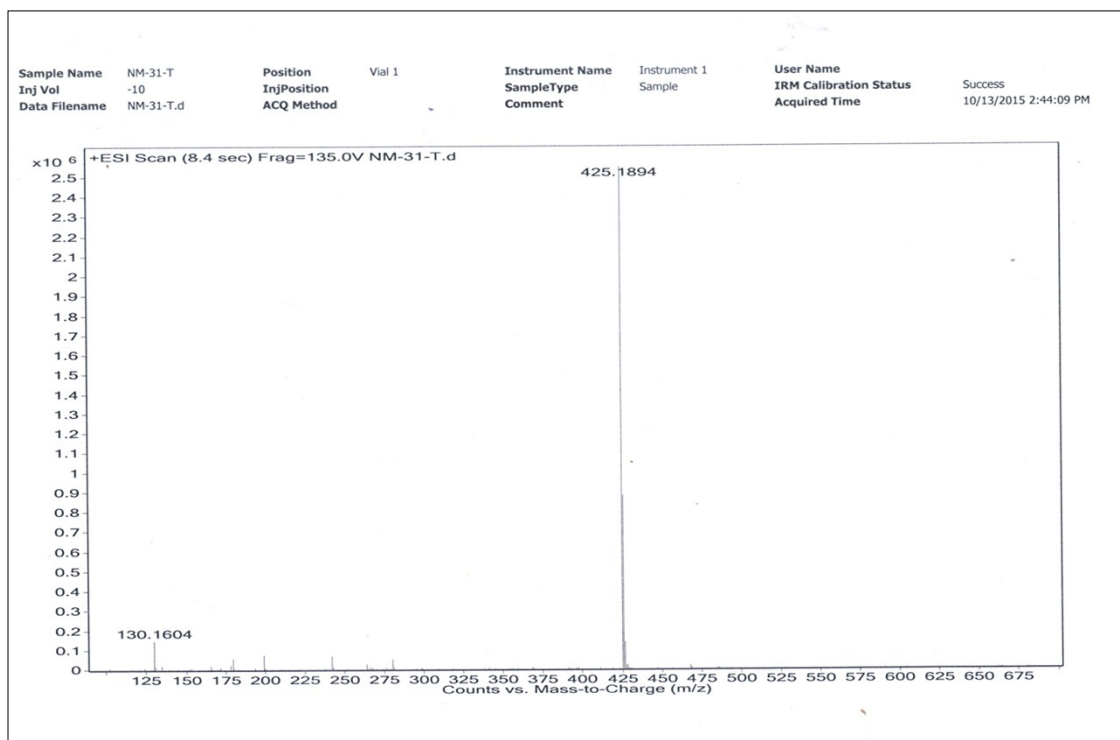
Mass Spectra of 6N



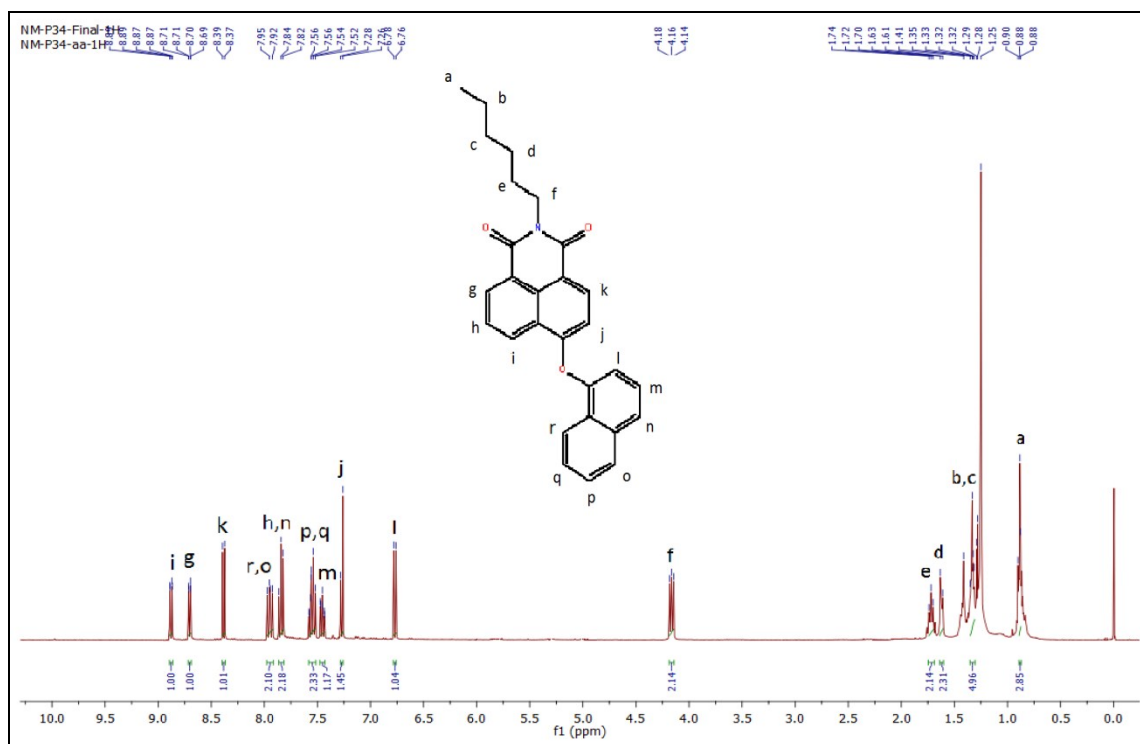
^1H NMR of α -NQ



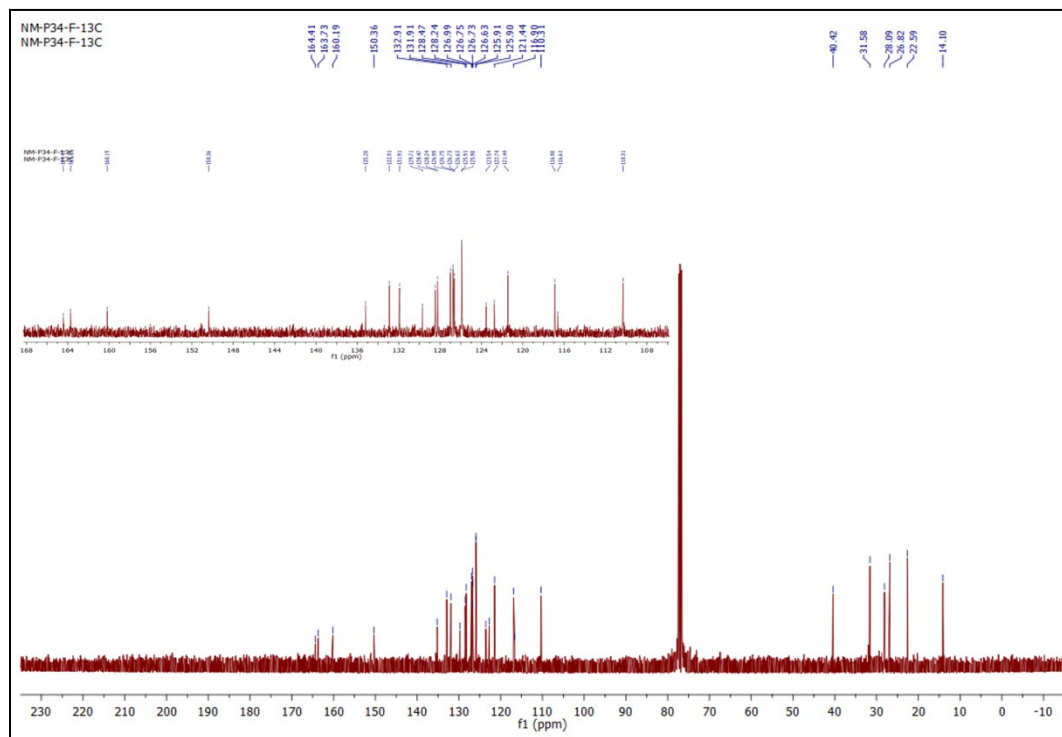
^{13}C NMR of α -NQ



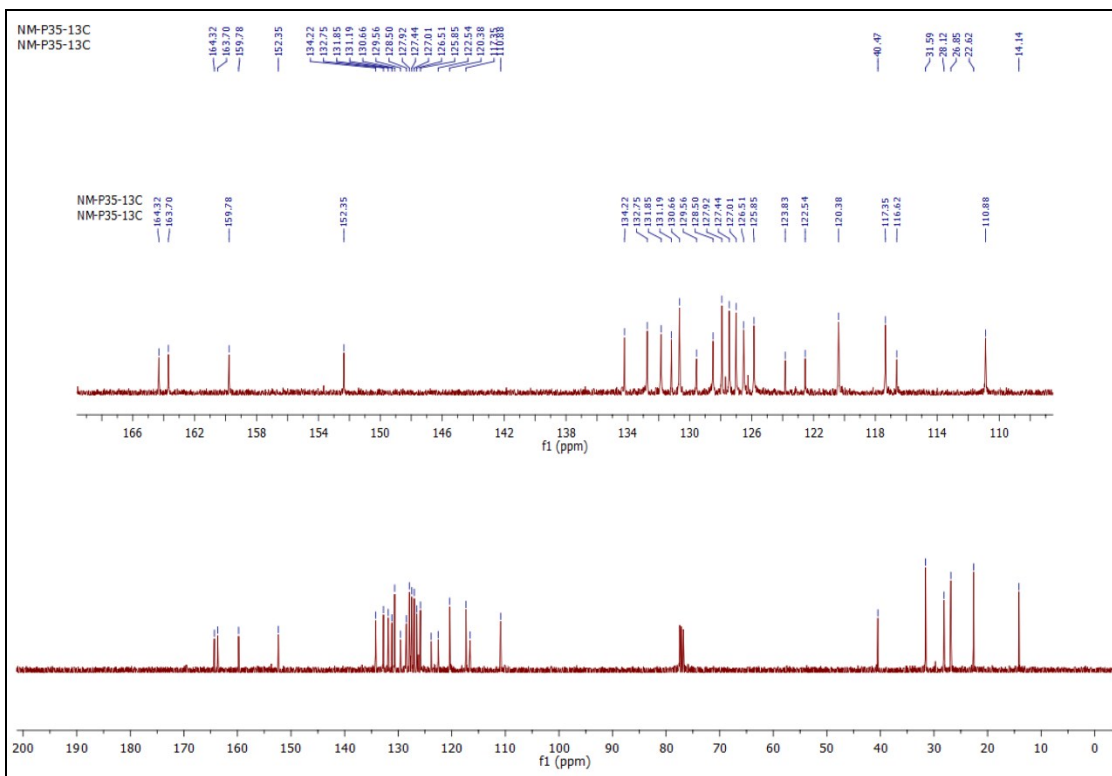
Mass Spectra of α -NQ



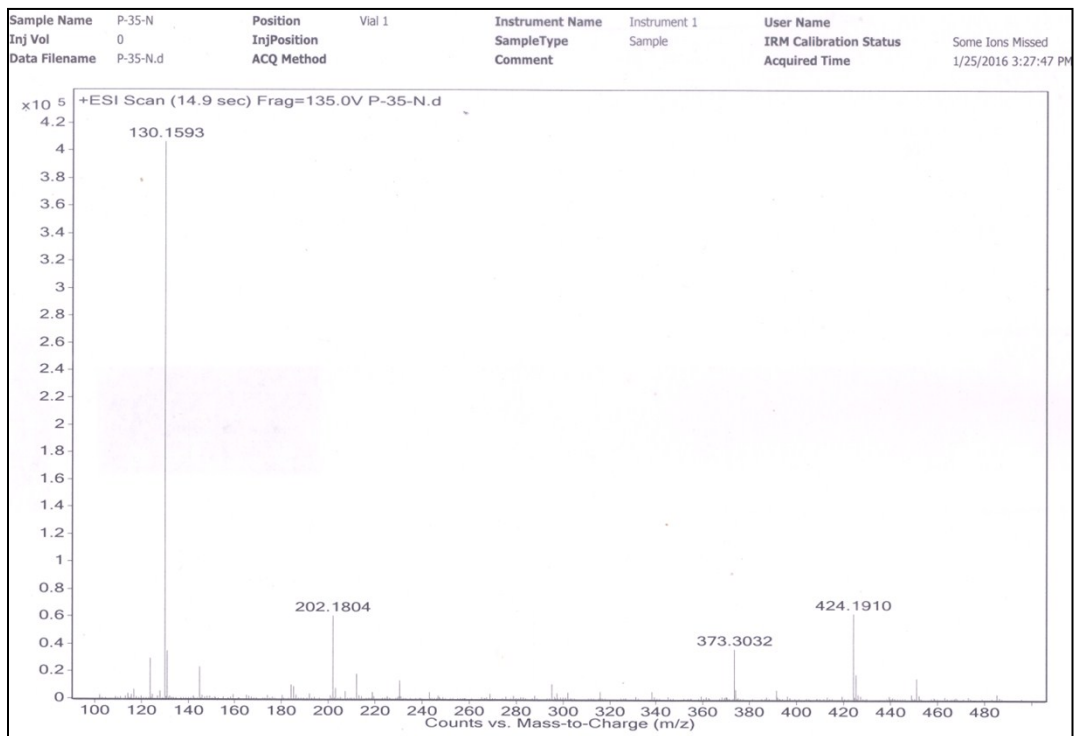
^1H NMR of α -NN



^{13}C NMR of α -NN



^{13}C NMR of β -NN



Mass Spectra of β -NN

11. References

1. G. M. Sheldrick, SAINT and XPREP, 5.1 edn, Siemens Industrial Automation Inc., Madison, WI, 1995.
2. G. M. Sheldrick, SHELX97. Program for X-ray Crystal Structure Solution and Refinement, University of Goettingen, Germany, 1997.
3. (a) C. Lee, W. Yang, and R. G. Parr, *Phys. Rev. B.*, 1988, **37**, 785–789; (b) A. D. Becke, *J. Chem. Phys.*, 1993, **98**, 5648–5652; (c) P. J. Stephens, F. J. Devlin, C. F. Chabalowski, and M. J. Frisch, *J. Phys. Chem.*, 1994, **98**, 11623-11627.
4. Gaussian 03, Revision E.01, M. J. Frisch, G. W. Trucks, H. B. Schlegel, G. E. Scuseria, M. A. Robb, J. R. Cheeseman, J. A. Montgomery, Jr., T. Vreven, K. N. Kudin, J. C. Burant, J. M. Millam, S. S. Iyengar, J. Tomasi, V. Barone, B. Mennucci, M. Cossi, G. Scalmani, N. Rega, G. A. Petersson, H. Nakatsuji, M. Hada, M. Ehara, K. Toyota, R. Fukuda, J. Hasegawa, M. Ishida, T. Nakajima, Y. Honda, O. Kitao, H. Nakai, M. Klene, X. Li, J. E. Knox, H. P. Hratchian, J. B. Cross, V. Bakken, C. Adamo, J. Jaramillo, R. Gomperts, R. E. Stratmann, O. Yazyev, A. J. Austin, R. Cammi, C. Pomelli, J. W. Ochterski, P. Y. Ayala, K. Morokuma, G. A. Voth, P. Salvador, J. J. Dannenberg, V. G. Zakrzewski, S. Dapprich, A. D. Daniels, M. C. Strain, O. Farkas, D. K. Malick, A. D. Rabuck, K. Raghavachari, J. B. Foresman, J. V. Ortiz, Q. Cui, A. G. Baboul, S. Clifford, J. Cioslowski, B. B. Stefanov, G. Liu, A. Liashenko, P. Piskorz, I. Komaromi, R. L. Martin, D. J. Fox, T. Keith, M. A. Al-Laham, C. Y. Peng, A. Nanayakkara, M. Challacombe, P. M. W. Gill, B. Johnson, W. Chen, M. W. Wong, C. Gonzalez, and J. A. Pople, Gaussian, Inc., Wallingford CT, 2004.
5. I. Fankuchen, *J. Biol. Chem.*, 1943, **150**, 57-59.